universität wien

DIPLOMARBEIT

Titel der Diplomarbeit

"Characterization of imatinib treated and untreated *CD4*-NPM-ALK and *CD4*-NPM-ALK-*CD4*$^{\Delta\Delta JUN}$ lymphomas regarding differences in stromal markers and motility proteins"

Verfasserin

Lena Amenitsch

angestrebter akademischer Grad

Magistra der Naturwissenschaften (Mag.rer.nat.)

Wien, 2013

Studienkennzahl lt. Studienblatt:	A 441
Studienrichtung lt. Studienblatt:	Diplomstudium Genetik - Mikrobiologie
Betreuer:	Ao. Univ.-Prof.Dr. Lukas Kenner (Medizinische Universität Wien)

Ein Wissenschaftler benötigt vier Dinge: erstens einen Kopf zum Denken; zweitens Augen zum Sehen; drittens Geräte zum Messen; und viertens - Geld.

Albert von Szent-Györgyi Nagyrápolt (1893-1986)

ABSTRACT

The anaplastic large cell lymphoma (ALCL) is a type of non-Hodgkin lymphoma that occurs more frequently in children and young adults. Overall, 40-60 % of ALCL cases show a chromosomal translocation, involving the nucleophosmin gene (*NPM*) and the membrane receptor anaplastic lymphoma kinase gene (*ALK*), which results in the expression of the chimeric NPM-ALK protein. By interacting with various adaptor proteins, the constitutively active NPM-ALK kinase induces cell transformation and increases cell proliferation. The AP-1 proteins JUN and JUNB were shown to be upregulated in human ALCLs. In a transgenic NPM-ALK mouse model, T-cell specific deletion on these factors led to a delay in tumor onset and reduced metastasis. Inhibition of the JUN/JUNB target PDGFRB by the tyrosine kinase inhibitor imatinib had similar effects on mouse survival as JUN/JUNB deletion. Here we show that tyrosine kinase inhibitors have growth inhibitory effects on murine ALK^+ NPM-ALK cell lines as well as on transplanted NPM-ALK tumors. Furthermore we could show that impairment of PDGFRB signaling in transgenic NPM-ALK mice by imatinib treatment or deletion of JUN/JUNB not only affects cancer cells, but also tumor stroma. Tumor vasculature and stromal components were significantly reduced in these lymphomas. We propose that both, lymphoma cells and tumor stroma, contribute to tumor progression in NPM-ALK mice and that in particular destabilization of the tumor vasculature in imatinib treated lymphomas might be the reason for the reduced tumor cell dissemination.

KURZFASSUNG

Das anaplastisch-großzellige Lymphom (ALCL) gehört zu den Non-Hodgkin-Lymphomen und tritt vor allem bei Kindern und Jugendlichen auf. Insgesamt zeigen 40-60 % der ALCL Fälle eine chromosomale Translokation, die durch die Fusion des Nukleophosmin-Gens (*NPM*) mit dem Anaplastische Lymphoma Kinase (*ALK*) – Gen entsteht und in der Expression des chimären NPM-ALK Proteins resultiert. Die konstitutiv aktive Tyrosinkinase NPM-ALK aktiviert verschiedene Signaltransduktionskaskaden und führt so zur neoplastischen Transformation und vermehrter Proliferation dieser Zellen. In einem transgenen NPM-ALK Mausmodell konnte gezeigt werden, dass T-Zell spezifische Deletion der AP-1 Faktoren JUN und JUNB zu einer Verzögerung der Tumorentstehung und verminderter Metastasierung führen. Weiters führt die Inhibierung des JUN/JUNB Zielgens *PDGFRB* durch den Tyrosinkinase-Hemmer Imatinib zu ähnlichen Resultaten. Mit dieser Arbeit konnten wir zeigen, dass Tyrosinkinase-Hemmer sowohl einen wachstumshemmenden Effekt auf murine ALK positive NPM-ALK Zelllinien, als auch auf transplantierte NPM-ALK Tumore haben. Weiters konnten wir zeigen, dass sich die Inhibierung des PDGFRB Signalweges in Tumoren von NPM-ALK Mäusen durch Behandlung mit Imatinib, bzw. durch Deletion von JUN/JUNB, nicht nur auf Krebszellen sondern auch auf stromale Faktoren auswirkt. In diesen Lymphomen waren sowohl Blutgefäße als auch stromale Komponenten deutlich reduziert. Wir nehmen an, dass sowohl Lymphomzellen als auch das Tumor Stroma zur Tumorprogression in NPM-ALK Mäusen beitragen und dass insbesondere die Destabilisierung der Blutgefäße in behandelten Lymphomen ein Grund für die verminderte Metastasierung sein könnte.

Table of Contents

Index of Figures

1 Abbreviations

ABL	V-abl Ableson murine leukemia viral oncogene homolog
ALCL	Anaplastic large cell lymphoma
ALK	Anaplastic lymphoma kinase
Alpha-SMA	Alpha-smooth muscle actin
AP-1	Activator protein 1
ARP2/3	Actin-related protein 2/3
ATP	Adenosin triphosphate
BAD	Bcl-2-associated death promotor
Bcl-2	B-cell lymphoma 2
Bcl-xl	B-cell lymphoma-extra large
BCR	Breakpoint cluster region protein
bFGF	Basic fibroblast growth factor
BSA	Bovine serum albumin
CAFs	Carcinoma associated fibroblasts
CHOP	Cyclophosphamide, Hydroxydaunorubicin, Oncovin, Prednisone
CLTCL	Clathrin heavy chain-like gene
CML	Chronic myelogenous leukemia
DAB	Diaminobenzidin
DFSP	Dermatofibrosarcoma protuberans
DMEM	Dulbecco’s modified eagle’s medium
DNA	Deoxyribonucleic acid
DTT	Dithiothreitol
ECM	Extracellular matrix
EDTA	Ethylenediaminetetraacetic acid
EGFR	Epidermal growth factor receptor
ELISA	Enzyme-linked immunosorbent assay
EMT	Epithelial-mesenchymal transition
ERK	Extracellular-signal-regulated kinase
EtOH	Ethanol
FAK	Focal adhesion kinase
FAP	Fibroblast activation protein
FOXO3a	Forkhead box O3a
GIST	Gastrointestinal stromal tumor
Grb2	Growth factor receptor-bound protein 2

HCl	Hydrogen chloride
HIV	Human immunodeficiency virus
ILK	Integrin-linked kinase
JAK	Janus Kinase
JNK	JUN N-terminal kinase
MAPK	Mitogen-activated protein kinase
MBS	Myosin light chain binding subunit
MLC2	Myosin II light chain
MLCK	Myosin light chain kinase
mTOR	Mammalian target of rapamycin
MYPT1	Myosin-binding subunit of myosin phosphatase 1
NaCl	Sodium chloride
NF-κB	Nuclear factor kappa-light-chain-enhancer of activated B-cells
NHL	Non-Hodgkin lymphoma
NK cells	Natural killer cells
NPM	Nucleophosmin
PAK	p21 activated kinase
PAS	Periodic acid-Schiff stain
PBS	Phosphate buffered saline
PCR	Polymerase chain reaction
PDGFRB	Platelet derived growth factor receptor beta
PI3K	Phosphatidylinositol-3-kinase
PKB	Protein Kinase B
PLC-γ	Phospholipase C-gamma
PTB	Phosphotyrosin-binding
ROCK1	Rho-associated, coiled-coil containing protein kinase 1
RPMI	Roswell Park Memorial Institute
RTK	Receptor tyrosine kinase
SCID	Severe combined immunodeficiency
SDS	Sodium dodecyl sulfate polyacrylamide
SH2	Src Homology 2
SPF	Specific pathogen-free
STAT3	Signal Transducer and Activator of Transcription 3
TAE	Tris-acetate-EDTA
TBST	Tris buffered saline with tween-20
TFG	TRK-fused gene

TGFβ	Transforming growth factor beta
TMP3	Tropomyosin 3
Tris	Hydroxymethylaminoethane
VEGF	Vascular endothelial growth factor
WASP	Wiskott-Aldrich syndrome protein
WAVE	WASP family verprolin-homologous protein
WHO	World Health Organization
WRC	WAVE2 Regulatory Complex

2 Introduction

2.1 Non-Hodgkin Lymphoma (NHL)

Lymphomas are cancers of the lymphatic system. Hodgkin's lymphoma accounts for about 10 % of all lymphomas and comprises two distinct types (classical and non-classical Hodgkin's lymphoma). Cancer cells of these patients are usually abnormal B-cells, called Reed-Sternberg (R-S) cells, which most often develop in lymph nodes located in upper body regions and spread to neighboring lymph nodes via lymphatic vessels.[2] The remaining 90 % are referred to as non-Hodgkin lymphoma. Non-Hodgkin lymphoma is the fifth most frequently diagnosed cancer in the UK, with roughly equal numbers of cases in men and women. It is more common in developed countries, with the United States and Europe having the highest rates. Over the last few decades incidence and mortality of non-Hodgkin lymphomas have been rising. More than two-thirds of patients are 60 years and older, but some types of lymphomas are more common in younger people. [3] About 85-90 % of NHL arise from B lymphocytes; the remainder derive from T lymphocytes or NK cells. Non-Hodgkin lymphomas usually develop in the lymph nodes, but can occur in almost any tissue and have a wide range of histological appearances and clinical features.[3,4] There are several classification systems that grouped NHL according to their histological characteristics; the most recent is the fourth editions of the WHO classifications 2008[1] (Table 1).

Non-Hodgkin lymphoma is linked with a number of risk factors, but the causes of most lymphomas are unknown. Some subtypes are associated with infection, for example, human T-lymphotropic virus in adult T-cell leukaemia and lymphoma or Epstein Barr virus in Burkitt's lymphoma. Immunosuppression is the most well established risk factor for the development of NHL. Patients with inherited immunodeficiency syndromes or autoimmune disease, as well as organ-transplant recipients and patients with HIV have an increased risk of developing a non-Hodgkin lymphoma.[3,4]

The genetic lesions involved in NHL include activations of proto-oncogenes and disruption of tumor suppressor genes. Chromosomal translocations represent the main mechanism of proto-oncogene activation in NHL and can be subdivided into 2 general groups.[5] An intact oncogene can be juxtaposed with another gene, usually an antigen receptor gene, and therefore becomes transcriptionally deregulated. Examples of this type is the (8;14) translocation in Burkitt's lymphoma.[6] The second type of chromosomal translocation results in a fusion gene and a novel protein. It is best known in acute and chronic myeloid leukemia [7-9] and occurs in some types of non-Hodgkin lymphomas, such as anaplastic large cell lymphoma (ALCL).[10-12]

	Diseases
B-cell lymphomas	
Precursor B cell	Precursor B-cell lymphoblastic leukaemia or lymphoma
Mature B cell	Chronic lymphocytic leukaemia/small lymphocytic lymphoma; lymphoplasmacytic lymphoma; splenic marginal-zone lymphoma; extranodal marginal-zone B-cell lymphoma of mucosa-associated lymphoid tissue; nodal marginal-zone B-cell lymphoma; follicular lymphoma; mantle-cell lymphoma; diffuse large B-cell lymphoma; Burkitt's lymphoma
B-cell proliferations of uncertain malignant potential	Lymphomatoid granulomatosis; post-transplantation lymphoproliferative disorders (polymorphic)
T-cell and NK-cell lymphomas	
Precursor T cell	Precursor T-cell lymphoblastic leukaemia or lymphoma
Extranodal mature T cell and NK cell	Mycosis fungoides; cutaneous anaplastic large-cell lymphoma; extranodal NK-cell or T-cell lymphoma; enteropathy-type lymphoma; hepatosplenic lymphoma; subcutaneous panniculitis-like lymphoma; primary cutaneous CD8-positive lymphoma; primary cutaneous γ/δ T-cell lymphoma; primary cutaneous CD4-positive lymphoma
Nodal mature T cell and NK cell	Peripheral T-cell lymphoma, not otherwise specified; angioimmunoblastic lymphoma; anaplastic large-cell ALK-positive lymphoma; anaplastic large-cell ALK-negative lymphoma; adult T-cell leukaemia/lymphoma

NK=natural killer.

Table 1. Subtypes of non-Hodgkin lymphoma according to the WHO classifications 2008[1] (Taken from Delsol, 2008)

2.2 Anaplastic Large Cell Lymphoma (ALCL)

Anaplastic Large Cell Lymphoma (ALCL) was initially described as a pleomorphic non-Hodgkin lymphoma characterized by large anaplastic lymphoid cells with uniform expression of cytokine receptor CD30 and a tendency to grow within lymph node sinuses.[13] Subsequent immunophenotypic and genetic studies showed that most ALCLs derive from the T-lineage.[14,15]

The current WHO classification[1] distinguishes three types of ALCL as separate disease entities: primary systemic ALK positive ALCL (ALK^+ ALCL), primary systemic ALK negative ALCL (ALK^-ALCL), and primary cutaneous ALCL.

Primary systemic ALK^+ ALCL cases are associated with chromosomal rearrangements of the anaplastic lymphoma kinase (ALK) gene and occur with a higher incidence in children and young adults when compared to ALK^-ALCL. In contrast to other systemic large-cell lymphomas, ALK^+ ALCLs appear to have a significantly better prognosis. Approximately 15-40% of ALCLs do not express ALK or other recurrent translocations and so far no recurrent cytogenetic alterations have been described in ALK^-ALCL. The molecular events responsible for the pathogenesis of this lymphoma are still largely unknown.[16]

Although systemic ALCL shows a broad spectrum of morphologic features, almost all cases share a common feature, which is the presence of a variable number of so called "hallmark cells".[17] These are large cells with abundant cytoplasm and eccentric lobulated "horse shoe" or kidney shaped" nuclei. Along with these characteristic cells, neoplastic elements with different morphology can be observed. In some cases nuclei are round and monomorphic and multinucleated cells may be present.

In addition to the common type ALCL (Fig. 1 c, 1d) which represents 75% of all cases, many variants have been described. Among these, the small cell variant (Fig. 1a) and the lymphohistiocytic variant (Fig. 1e) are the most common and important.[17]

Approximately 75% of ALK^+ ALCLs are associated with a balanced t(2;5)(p23;q35) translocation which generates the oncogenic fusion-protein NPM-ALK (nucleophosmin - anaplastic lymphoma kinase).[18] In the remaining cases *ALK* is fused to a number of variant partner genes such as *TPM3* (tropomysin 3), *TFG* (TRCK fusion gene), *ATIC* and *CLTCL*.[19]

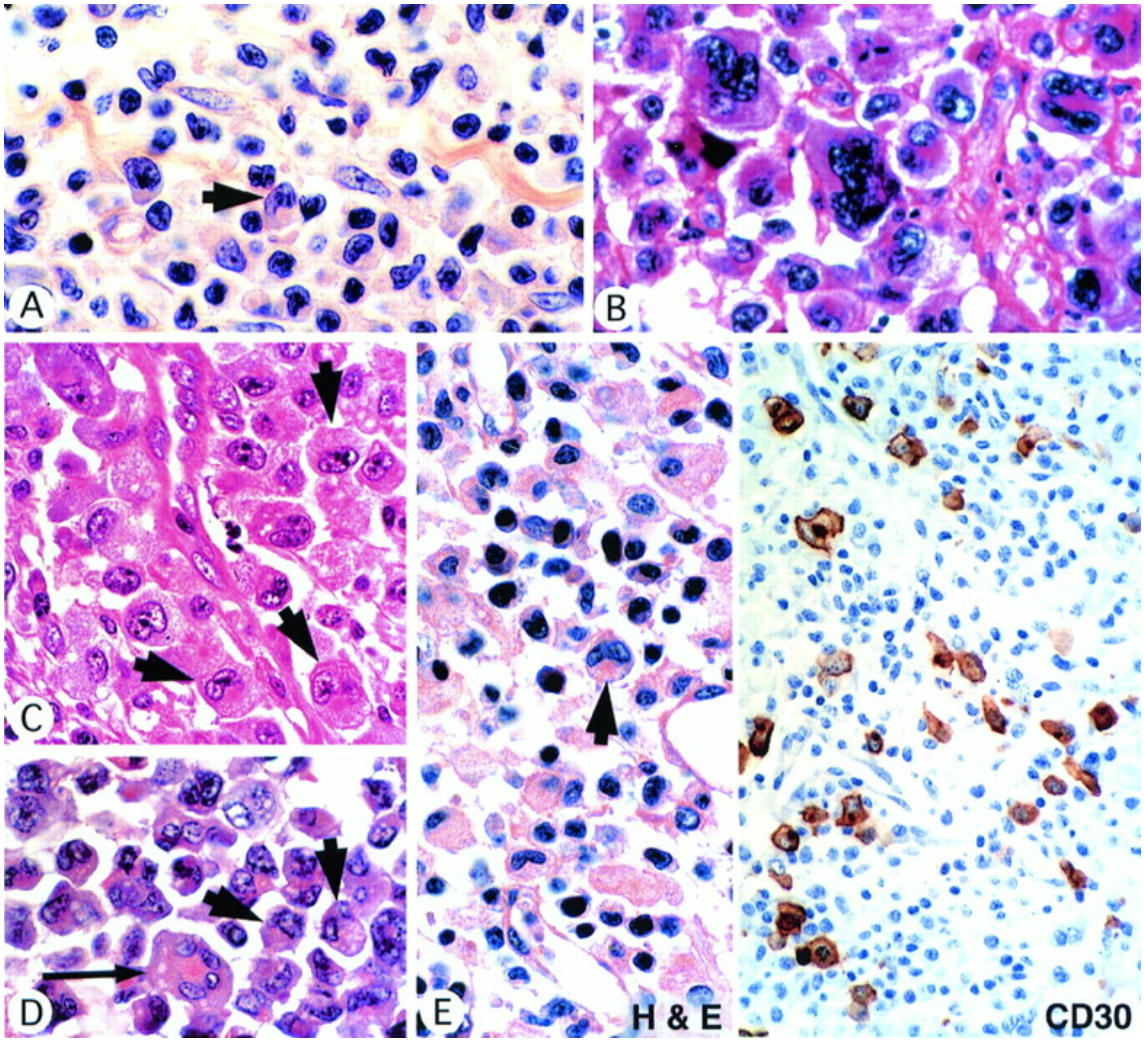

Figure 1. **ALCLs show a wide morphologic spectrum.** (A) Predominant population of small cells associated with large hallmark cells (arrow) (B) Giant-cell–rich pattern (C)(D) Common-type ALCL showing several hallmark cells (arrows) (E) Lymphohistiocytic variant. (Taken from Benharroch et al., 1998)

With the standard therapy for T-cell lymphomas, CHOP (type) chemotherapy (cyclophosphamide, doxorubicin, vincristine, and prednisone) the cure rate of ALK^+ ALCLs reaches 60-80 %.[16] However, some patients do not respond to therapy or experience chemo-resistant relapses. Recent research reveals that the ALK protein is an ideal antigen for vaccination strategies as its wild type expression is low and restricted to few cells. Furthermore a few small-molecule inhibitors of ALK kinase activity have been described: Crizotinib (Xalkori, Pfizer) was approved in 2011 by the U.S. Food and Drug Administration for treatment of ALK-positive non-small-cell lung cancer (NSCLC).[20] Crizotinib is also being tested in clinical trials of Systemic Anaplastic Large-Cell Lymphoma at present. Another small-molecule inhibitor of ALK, NVP-TAE684, was shown to block the growth of ALK^+ ALCL cell lines and to suppress lymphomagenesis ALK^+ ALCL mouse models.[21]

Recently PDGFRB blockade could be shown to be a highly effective therapy for NPM-ALK^+ ALCL.[22] Furthermore the characterization of deregulated microRNAs provides starting points for future therapies of ALCL.[23]

2.2.1 NPM-ALK

The most common chromosomal aberration in Systemic Anaplastic Large Cell Lymphomas is the (2;5)(p23;q35) translocation resulting in overexpression of a chimeric oncogene, nucleophosmin-anaplastic lymphoma kinase (NPM-ALK). NPM-ALK plays a key role in ALCL lymphomagenesis and cause lymphoid malignancy *in vitro* and *in vivo*.[24]

The anaplastic lymphoma kinase (ALK) is an orphan receptor tyrosine kinase and was first identified as a part of the translocation in ALCL.[18] Because of its significant homology to the leukocyte tyrosine kinase [25], ALK is placed in the insulin receptor superfamily of RTKs. The fully matured glycosylated protein weighs 220 kDa and is normally expressed only within the developing and mature nervous system; it is not expressed in normal lymphoid cells.[25,26] The function of ALK and how it is physiologically activated is not completely known.

NPM is an ubiquitously and highly expressed 37 kDa phosphoprotein, which exists in cells as a homohexamer and plays a role in ribosome assembly. Its functions include the shuttling of ribonuclear complexes between the nucleolus and the cytoplasm.[27,28]

In the (2;5) translocation, the chromosomal breakpoints consistently fall within intron 4 of NPM and intron 16 of ALK, producing a *NPM-ALK* gene on the chromosome 5 derivative and a *ALK-NPM* gene on the chromosome 2 derivative (Fig. 2).

But hence only the *NPM* promoter is active in lymphoid cells, only the product of the *NPM-ALK* fusion gene can be detected in lymphoma cells.[18,29] This 80 kDa fusion protein consists of the catalytic part of ALK fused to the N-terminal region of NPM, which contains the oligomerization domain. This domain drives the homodimerization of NPM-ALK which results in autophosphorylation and constitutive activation of the ALK tyrosine kinase.[30] The truncated NPM also contains a nucleolar localization domain, which explains why the NPM-ALK protein in contrast to other ALK fusions can be detected in the cytoplasm, nucleus and nucleolus.[19]

The transforming ability of NPM-ALK which was repeatedly shown *in vitro* [30] and the development of malignant lymphomas in transgenic mouse models [24] demonstrate the oncogenic properties of NPM-ALK. NPM-ALK has been shown to interact with various molecular factors, which are probably also involved in the development of the lymphoma with its characteristic features.[31]

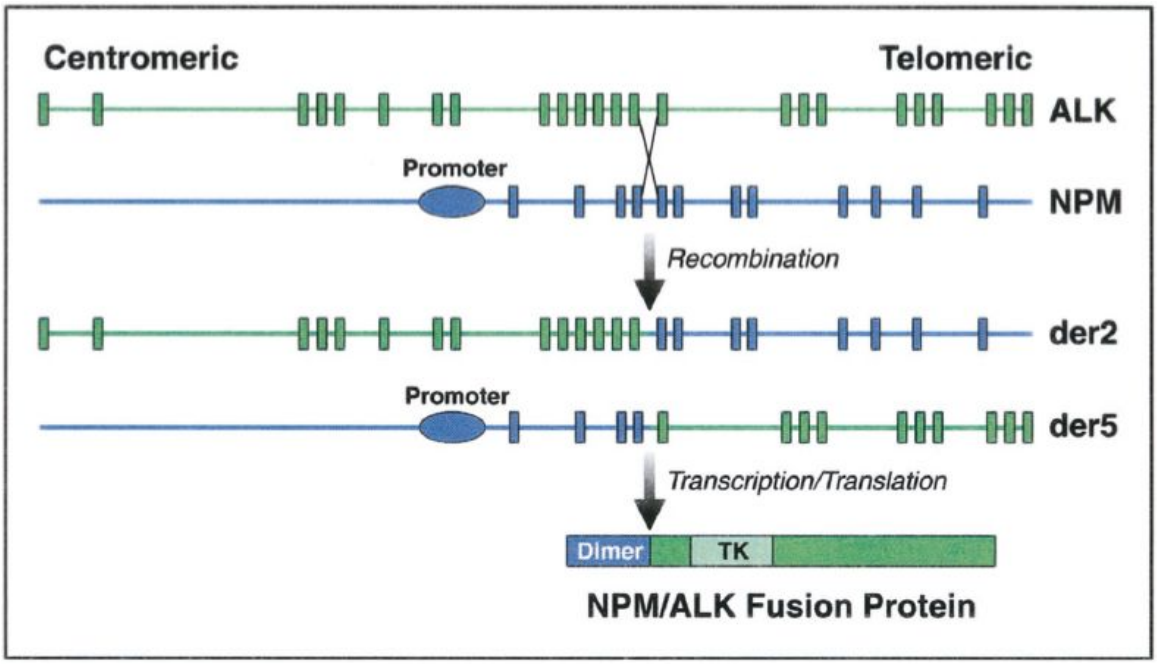

Figure 2. Structure of *NPM, ALK*, and *NPM-ALK* genes. (Taken from Amin et al., 2007)

2.2.2 Signals downstream of activated ALK

The homodimerization of NPM-ALK fusion proteins, which is managed by the NPM domain, dramatically increases autophosphorylation of multiple tyrosine residues within the ALK portion of the protein. An ensemble of proteins with SH2 or PTB domains binds to the phosphorylated residues and thus couples the NPM-ALK protein to downstream signaling pathways regulating mitogenesis and survival. As many as 46 proteins were identified to selectively associate with NPM-ALK, indicating a complex signalosome in which adaptors probably compete for binding to the same phosphotyrosine residue.[32]

Activation of STAT3, AKT/PI3K and RAS/ERK pathways, which control cell proliferation, survival and cell cycling, are the most important effects of ALK kinase activity.[33-36]

In addition to the antiapoptotic effects of PI 3-kinase signaling via BAD phosphorylation[34], the kinase appears to play a role in mediating NPM-ALK induced mitogenesis by acting on cell-cycle regulation. FOXO3a is phosphorylated by Akt and promote cell cycle progression.[37] Furthermore the sonic hedgehog signaling pathway is mediated by NPM-ALK through activation of PI3K/AKT. Inhibition of this pathway induces apoptosis and cell cycle arrest.[38]

Activated STAT3 could be detected in many ALK^+ALCL tumor samples as well as in cell lines and tumor tissues of NPM-ALK transgenic mice. [39-41] NPM-ALK mediated STAT3 activation has been shown to mediate both survival and proliferative signals. Survival signals include upregulation of antiapoptotic factors such as Bcl-2 and Bcl-xl.[42] Positive regulators of G1 cell-cycle progression such as cyclin D3 and c-Myc are upregulated in tumor tissues from transgenic mice.[39]

The Ras-MAPK pathway, which is supposed to be activated as a result of the recruitment of Grb2 and Shc to the NPM-ALK signalosome, contributes to increased proliferation of ALCL cells. Depletion of ERK1/2, which was found to be highly phosphorylated in tumor cells derived from NPM-ALK transgenic mice [39], impairs cell proliferation and induces apoptosis.[43] Together with JNK MAP kinase pathway, which is also active in tumor tissues [44], ERK pathway promote actions of downstream transcription factors such as members of the activator protein-1 family (AP-1). These factors initiate the transcription of growth promoting proteins and regulators of apoptosis.[45]

Activation of CD30 in NPM-ALK expressing lymphomas can be attributed to the constitutively active MAPK/JUNB signaling cascade and activated STAT3. It results in cell cycle arrest and apoptosis through activation of the NF-κB pathway.[46]

PLC-γ binds directly, via an interaction at tyrosine residue 664, to NPM-ALK. Replacement of Tyr664 abrogated the transforming potential, suggesting an important role of PLC-γ in NPM-ALK oncogenic signaling.[47]

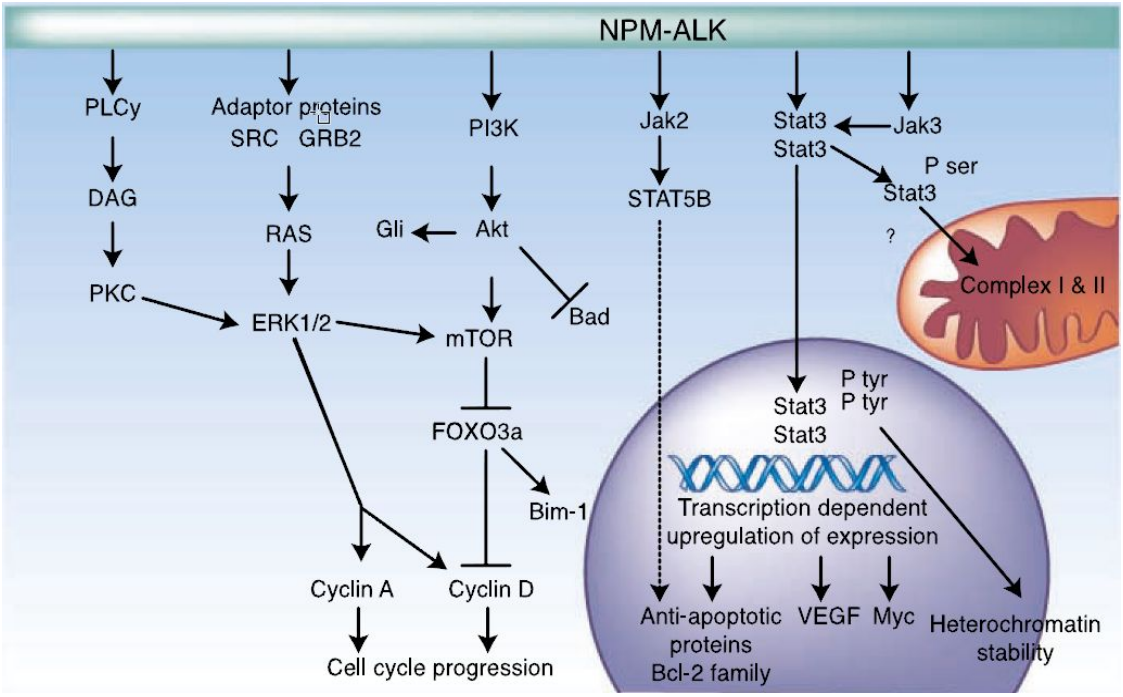

Figure 3. Signals generated by the NPM-ALK fusion protein. NPM-ALK activates PLCγ, Ras, STATs, JAKs and PI3K/Akt pathway. (Taken from Mossé et al., 2009)

2.2.3 Activator protein 1 (AP-1)

The activator protein 1 (AP-1) is a dimeric transcription factor and belongs to the basic leucine-zipper group of DNA binding proteins. AP-1 induces the transcription of numerous target genes, thereby regulating a wide range of cellular processes including cell proliferation, death, survival and differentiation.[45,48] The JUN (JUN, JUNB, JUND) and FOS (FOS, FOSB, FRA1, FRA2) subfamilies are the main AP-1 proteins in mammalian cells and JUN and FOS were first identified as viral oncoproteins. AP-1 can consist of many different combinations of homo- and heterodimers, which determines its binding specificity and affinity.[49] Its activity is regulated on the one hand at the level of expression, in response to a number of stimuli such as cytokines, growth factors, stress, infection and on the other hand by post-translational modification of the different subunits.[50,51] The best characterized member of the AP-1 family, JUN, has a growth promoting activity which is mediated through transcriptional activation of cell cycle regulators such as cyclins, as well as suppression of p53 and cyclin-dependent kinase inhibitors such as $p19^{ARF}$ and $p16^{Ink4}$.[52,53]

The function of JUNB in neoplastic transformation is complex and could be either proapoptotic or antiapoptotic, depending on the cellular context. JUNB, which was shown to be overexpressed in $CD30^+$ lymphomas [36,54], is suggested to be the main AP1 transcription factor involved in the pathogenesis of ALCL. Its expression appears to be more abundant in NPM-ALK-positive cell lines in contrast to NPM-ALK-negative ALCL cells. JUNB enhances cell cycle progression in NPM-ALK ALCL; it is transcriptionally activated via ERK1/2 and translationally regulated via mTOR signaling.[55]

Studies have shown that JUN is also highly expressed in CD-30 positive lymphomas including ALK^+ALCL.[36,56] NPM-ALK phosphorylates and activates the MAPK JUN N-terminal kinase (JNK), which in turn phosphorylates and activates JUN. Activation of JUN results in increased JUN transcriptional activity on target cell-cycle regulatory genes.[57] AP-1 also plays a role in tumor invasion, primarily JUN-FOS complexes are supposed to regulate genes important for tumor metastasis.[58] In a cell culture model of fibrosarcoma JUN and JUNB were found to be upregulated during tumor progression and increase angiogenesis by activation of the angiogenic factor proliferin.[59]

2.2.4 Platelet derived growth factor receptor beta (PDGFRB)

Platelet derived growth factors (PDGF) have important functions during development, cell growth, proliferation and differentiation, blood vessel formation and are involved in a wide range of diseases.[60] The PDGF family consists of four different isoforms, PDGF-A, -B, -C and –D, which can form either homo- or heterodimers and bind to their receptors PDGFRA and PDGFRB. The receptor isoforms dimerize upon binding of the PDGF dimer, leading to three possible receptor combinations (αα, ββ, αβ). Among the multiple possible PDGF-PDGFR interactions, which have been demonstrated *in vitro*, only few interactions could be proven *in vivo*: PDGF-AA and PDGF-CC via PDGFRA and PDGF-BB via PDGFRB.[61]

The dimerization of the receptor leads to activation of the intrinsic tyrosine kinase domain and subsequent recruitment of SH-2-domain-containing signaling proteins.[62,63] PDGFRA and PDGFRB activate important signaling pathways like MAPK, PI3K and PLC-γ, leading to growth stimulation, differentiation, actin reorganization, migration and inhibition of apoptosis.[64-66] Studies revealed that PDGFRA signaling plays an important role in animal development, in particular in gastrulation and development of the neural crest, gonads, lung, intestine, skin, CNS and skeleton. PDGFRB signaling is essential for blood vessel formation and early hematopoiesis.[67,68] There is limited evidence for normal physiological functions of PDGFs in the adult. PDGF signaling has been linked with several diseases and pathological conditions. PDGF signaling seems to play a role in tumor cell growth, tumor angiogenesis, tumor fibroblast growth and invasion and metastasis of certain epithelial cancers.

2.2.5 Transgenic NPM-ALK mouse model

The group around Lukas Kenner, which I joined as a Diploma student, is working with transgenic mice carrying the human NPM-ALK cDNA under the control of a murine *CD4* promotor.[39] They crossed these mice, which develop T-cell lymphomas around 8 weeks after birth, with mice carrying loxP-flanked versions of *JUN* and/or *JUNB* [69,70], as well as with mice carrying *CD4*-Cre [71] (Fig. 5a).The specific deletion of *JUN* and *JUNB* in T-cells resulted in a significantly delay in tumor onset, reduced proliferation and enhanced apoptosis of tumor cells [22] (Fig. 5b, 5c).

Lymphoma cells from *CD4*-NPM-ALK mice showed strong expression of PDGFRB and pPDGFRB, whereas the expression in *CD4*-NPM-ALK-*CD4*$^{\Delta\Delta JUN}$ lymphomas was nearly entirely absent. PDGFRB could be identified as novel direct target of JUNB and JUN (Fig.4).

Impairing PDGFRB activity with the FDA approved PDGFR kinase inhibitor imatinib was shown to significantly prolong survival time of NPM-ALK mice (Fig. 6a), as well as to strongly reduce tumor growth of transplanted NPM-ALK tumors (Fig. 6b).

Lymphoma cells in the NPM-ALK mouse model spread into many organs.[39] Massive hepatic infiltration of lymphoma cells, as well as tumor cells invading blood vessels of portal veins of liver parenchyma, could be detected in *CD4*-NPM-ALK mice. In *CD4*-NPM-ALK-*CD4*$^{\Delta\Delta JUN}$ lymphomas no dissemination of tumor cells to the liver or other organs could be found [22] (Fig. 7).

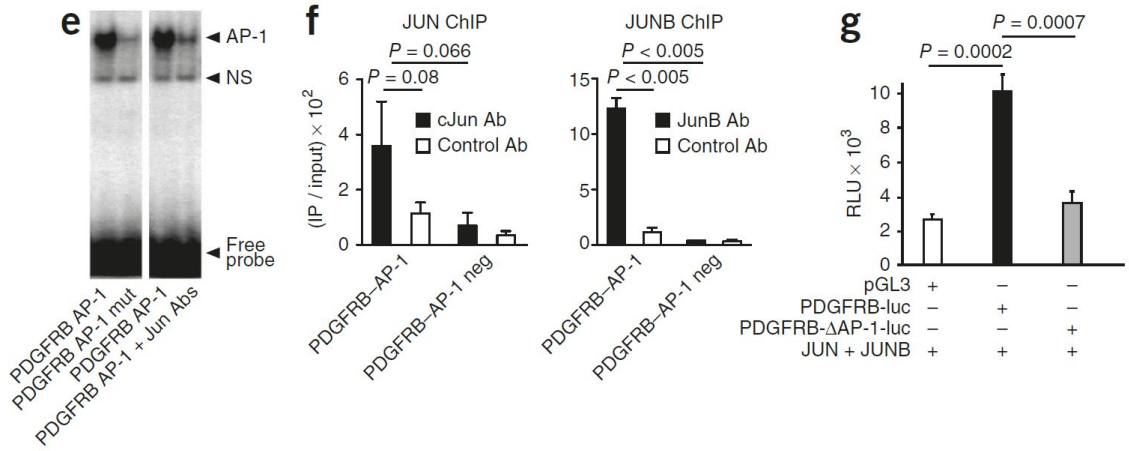

Figure 4. PDGFRB is a direct transcriptional target of JUNB and JUN. (e) Electrophoretic mobility shift assay analysis using a conserved PDGFRB AP-1 site (PDGFRBAP-1) and a mutated version (PDGFRBAP-1 mut). (f) Chromatin immunoprecipitation (ChIP) using antibodies to JUN and JUNB in the human fibroblast cell line BJ-1. (g) Luciferase reporter assay to determine functionality of the AP-1 site for PDGFRB promoter regulation. pGL3, promoterless luciferase vector (control); pPDGFRB-luc, luciferase vector with PDGFRB promoter; pPDGFRB-ΔAP-1-luc, luciferase vector with PDGFRB promoter lacking AP-1 site; pJUN + pJUNB, JUN and JUNB expression vectors. (Taken from Laimer et al., 2012)

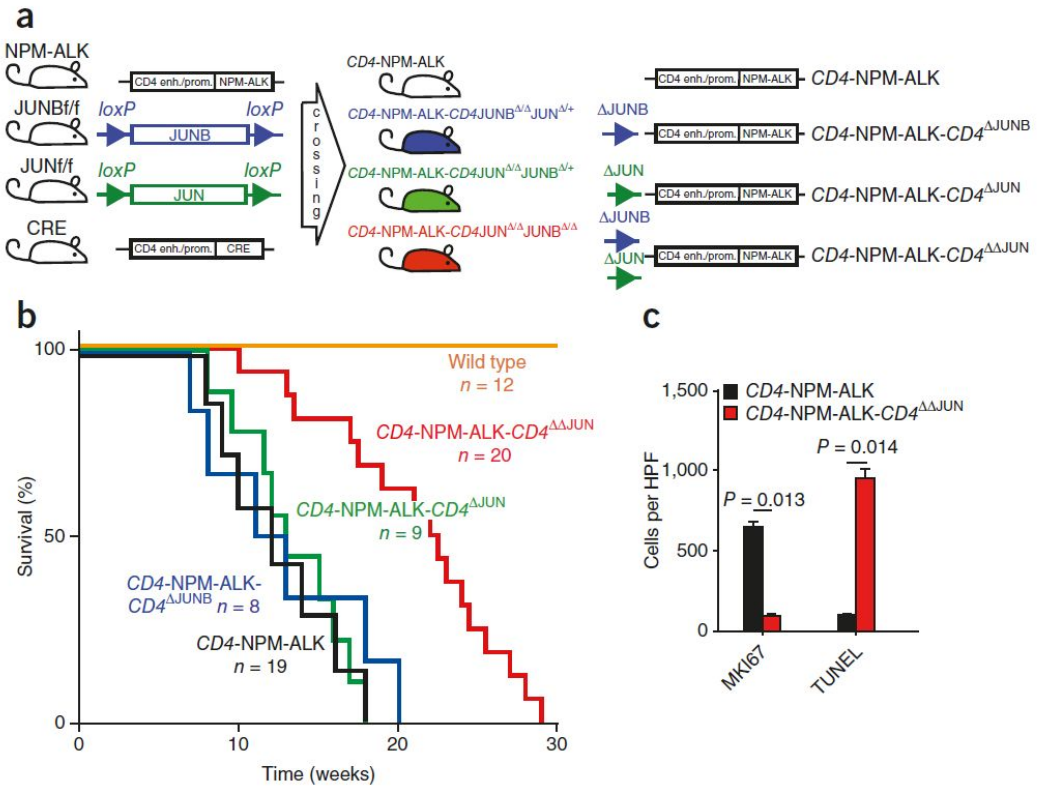

Figure 5. Effects of JUN and JUNB deletion on NPM-ALK lymphomas in mice.

(a) Generation of mouse strains (b) Kaplan-Meier curves depicting overall survival of mice. (c) Assessment of apoptosis and proliferation in sections of *CD4*-NPM-ALK and *CD4*-NPM-ALK-*CD4*$^{\Delta\Delta JUN}$ lymphomas. (Taken from Laimer et al., 2012)

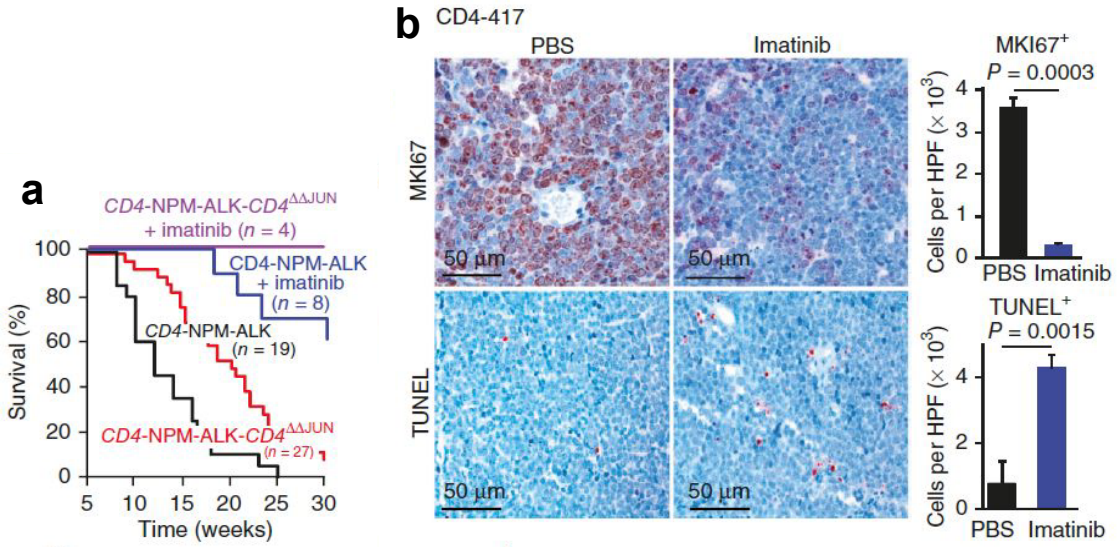

Figure 6. (a) Survival curves of imatinib-treated and untreated *CD4*-NPM-ALK and *CD4*-NPM-ALK-*CD4*$^{\Delta\Delta JUN}$ mice. (b) Proliferation and apoptosis in transplanted lymphoma cells. (Taken from Laimer et al., 2012)

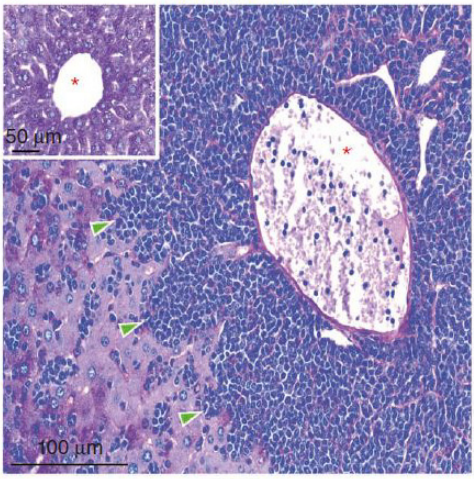

Figure 7. PAS (Periodic acid Schiff) staining in the liver from *CD4*-NPM-ALK-*CD4*$^{\Delta\Delta JUN}$ (small inset) and *CD4*-NPM-ALK mice. Green arrowheads denote tumor cells in the liver parenchyma of *CD4*-NPM-ALK mice; red asterisks denote blood vessels. (Taken from Laimer et al., 2012)

2.2.6 Tumor stroma and PDGFRB

Most tumors grow as solid masses and have a distinct structure that consists of two compartments: the parenchyma (neoplastic cells) and the stroma [72]. The stroma is formed by elements that are derived from the circulating blood and from host connective tissue and plays a role in processes such as the support of nutrients and oxygen, the removal of products from the growing tumor and the creation of a barrier regulating the interchange of cells, fluid and gases [73,74]. The major components of tumor stroma include blood vessels, plasma and plasma proteins, proteoglycans and glycosaminoglycans, interstitial collagens, fibrin, fibronectin, connective tissue cells and inflammatory cells.[75] Tumors differ considerably from each other in stromal content. In desmoplastic tumors, such as many carcinomas of the breast, pancreas and stomach, up to 90 % or more of the total tumor mass consists of stroma.[75] Contrarily most medullary carcinomas of the breast have a minimal stroma part.[76] The composition of tumor stroma also varies from tumor to tumor. The phenotype of a tumor can be determined by the interaction between the cancer cells and their microenvironment. Cancer cells can produce stroma-modulation growth factors, such as bFGF (basic fibroblast growth factor), members of the VEGF (vascular endothelial growth factor) family, PDGF (platelet-derived growth factor, EGFR (epidermal growth factor receptor) ligands, interleukins and TGFβ (transforming growth factor-β). These factors activate surrounding stromal cell-types and induce stromal reactions, such as the inflammatory response and angiogenesis.[75,77] To grow beyond a critical site or metastasize to another organ, tumors must recruit new blood vessels by vasculogenesis and angiogenesis. Various signals trigger the angiogenic switch, including metabolic and mechanical stress, immune response and genetic alterations.

It is largely unknown, how the interplay between genetic and environmental mechanisms influences tumor angiogenesis and tumor growth. Tumor angiogenesis is regulated by pro- and anti-angiogenic molecules that come from cancer cells, stromal cells, endothelial cells, blood and the extracellular matrix. Their relative contribution depends on the tumor type and tumor site and changes with tumor growth and regression.[78]

PDGFRB plays a major role in tumor angiogenesis; in particular it stimulates pericyte recruitment to tumor capillaries.[79] This is mediated by PDGF-receptors expressed on pericytes, which are activated by PDGF-BB or PDGF-DD. PDGFRB positive pericytes were found in more than 90 % of samples of a tumor tissue array comprising colon, breast, lung and prostate cancer and could be also demonstrated by confocal analyses of capillaries in human colon cancer.[80,81] Pericytes are embedded in the basement membrane of microvessels and promote stabilization and maturation of newly formed vessels. Pericytes surrounding normal capillaries are well-organized and closely attached with endothelial cells. Recent studies using confocal microscopy showed that tumor pericytes had a lower density and a looser connection with endothelial cells.[82,83] Studies have demonstrated that forced PDGF overproduction by tumor cells is associated with increased pericyte abundance[84,85] and even leads to an increased tumor growth rate and reduced tumor cell apoptosis, which was shown in the B16 mouse melanoma model.[86]

In several tumor types including colectoral cancer and small-cell lung carcinoma, PDGF is also involved in paracrine stimulation of stroma cells. It plays a crucial role in recruitment of tumor fibroblasts, which contribute to tumor progression and tumor angiogenesis. Fibroblasts were first thought to be passive participants in neoplastic programming, but recent data show that they have an active role[87] and even can promote neoplastic programming of tissue.[88] Fibroblasts are responsible for the synthesis, deposition and remodeling of the ECM, as well as for the production of paracrine growth factors that regulate cell proliferation, morphology, survival and death. Tumor fibroblasts, also referred to as myofibroblasts or CAFs (carcinoma-associated fibroblasts), are large spindle-shaped mesenchymal cells that share characteristics with smooth-muscle cells and fibroblasts. They express a combination of different markers, such as α-smooth muscle actin, vimentin, desmin and fibroblast activation protein (FAP)[89]. Myofibroblasts are surrounded by dense accumulations of fibrillar collagens and exhibit a higher proliferative index, as compared with normal fibroblasts. This phenotype is called desmoplasia and is associated with activation of angiogenic programs and recruitment of inflammatory cells.[90] CAFs were found in the activated tumor stroma of different types of cancer, such as breast cancer, prostate cancer, lung cancer and colon cancer.[91,92]

TGFβ and PDGF are secreted by a range of tumor cells and were shown to be the main inducers of desmoplasia, through their effect on stromal fibroblasts.[93-95] Immunohistochemical studies have shown PDGFRB expression in the stroma of various tumor types, e.g. breast cancer, lung cancer, ovarian cancer and pancreatic cancer.[96-99] A study has demonstrated that PDGF-driven recruitment of fibroblasts converted immortal human keratinocytes from a nontumorigenic to a tumorigenic phenotype.[100] Xenotransplanted human melanoma cells producing PDGF-BB formed stroma rich and highly vascularized tumors in contrast to tumor cells which reduced PDGF production, demonstrating the potential role of PDGF in stroma development.[101]
In epithelial cancers PDGF expression is suggested to play a role inn EMT and tumor dissemination. It was demonstrated that autocrine PDGF signaling maintains EMT and promotes metastasis in mouse mammary carcinoma.[102] In human breast carcinoma, expression of PDGF has been found to correlate with advanced tumor stages and unfavorable prognosis.[103] Members of the PDGF family were also shown to display direct potent lymphangiogenic activity. Expression of PDGF-BB in murine fibrosarcoma cells induced tumor lymphangiogenesis, leading to enhanced metastasis in lymph nodes.[104]

2.2.7 Metastasis

Non-Hodgkin lymphomas predominantly involve the lymph nodes, but may affect other organs. The most frequent sites of secondary lymphomas are the bone marrow and the liver.[105] In a histopathological study, neoplastic infiltration of the liver was observed in nearly 50 % of samples from untreated lymphoma and leukaemia patients.[106] The metastatic behaviour of lymphoma cells is probably based on mechanisms of migration of normal lymphocytes. Lymphocytes can be activated by various stimuli. They start to extend pseudopodia and acquire a polarized shape. The molecular events that contribute to cell motility are very complex. Many proteins, including receptor, crosslinking, binding, adhesion and motor proteins are involved in the determination of the direction of cell movement. The crawling of the cell is primarily driven by actin polymerization and acto-myosin contractility.[107] It is known that active cell movement contributes to invasion and metastasis of most neoplastic cells. Studies provide statistical evidence for the correlation between cell motility parameters and malignant behaviour of cancer cells.[108] In a murine T-cell lymphoma study, malignant cells were compared to non-malignant cells regarding motility and F-actin content. Metastatic, invasive variants of lymphoma cell lines performed active shape changes by protruding and retracting pseudopodia in contrast to noninvasive cell lines.

It was shown that a high level of actin polymerization is prerequisite for the formation of pseudopodia, which are necessary for infiltration of the cells into tissues.[109]

Motility proteins

The process of cell motility consists of four major steps: formation of protrusions at the leading edge, formation of new adhesions, cell body contraction and deadhesion.[110] Many proteins are involved in this process; some of them will be described below.

ERK1/2

In addition to its role in the control of proliferation and cell death, there is growing evidence that ERK MAPK signaling is implicated in the regulation of cell motility. ERK contributes to the formation of cellular protrusions by regulating the small GTPases Rac1 and RhoA. Furthermore the ERK MAPK pathway facilitates the process of cell migration through direct cytosolic activation of protease calpain-2 and MLCK, contributing to cell adhesion turnover.[111]

Paxillin

Paxillin is a multidomain adaptor located at the interface between the actin cytoskeleton and the plasma membrane. It serves as linkage for multiple regulatory and structural proteins, which control cell adhesion, cytoskeletal reorganisation and gene expression necessary for cell migration and survival.[112] Paxillin is a regulator of the Rho family of small GTPases, which includes Rac1, RhoA and Cdc42. By stimulating actin-stress-fiber formation, RhoA plays a role in cell contractility and translocation. Cdc42 is required for the formation of filopodia and cell polarization, whereas Rac1 promotes the extension of lamellipodia.[113] JNK phosphorylation of paxillin has been implicated as critical for cell motility.[114] Additionally paxillin was found to play an essential role in adhesion mediated activation of ERK.[115]

ROCK1

Rho-associated kinases belong to a family of serine/threonine kinases and have been identified as key downstream effectors of Rho GTPases. They are involved in many aspects of cell motility.[116] Two ROCK isoforms have been identified: ROCK1 and ROCK2.[117] Although their functional differences are poorly understood, it is suggested that they contribute to increased actin-myosin II mediated contractility. They directly phosphorylate myosin light chain and negatively regulate myosin light chain phosphatase.[118,119]

ARP2/3

The actin-related protein-2/3 (ARP2/3) complex has been shown to play a crucial role in the formation of branched-actin-filament networks during diverse processes.

It is a central player in the regulation of the initiation of actin polymerization and the organization of the resulting filaments. The complex consists of two actin like and five additional proteins and is regulated by its association with WAVE and WASP family proteins. They bring actin monomers very close in proximity to the ARP2/3 complex, thereby increasing the rate of actin polymerization. Members of the Rho GTPase family are also implicated in the recruitment and activation of the ARP2/3 complex.[120]

MLC2

Protein complexes that consist of F-actin and myosin II filaments use energy from ATP hydrolysis to power actin-myosin contraction. A key mechanism for the regulation of the contractility is the phosphorylation of the myosin II light chains (MLC2).[121] It facilitates the association of the myosin head with F-actin and allows the myosin heavy chain tail to assemble into filaments. MLC phosphorylation can be mediated by various kinases including ROCK1, ROCK2, ILK, PAK and MLCK.[118,122] The dephosphorylation of MLC is catalyzed by a phosphatase complex that consists of a catalytic subunit, a myosin light chain binding subunit (MBS) and a smaller subunit of unknown function.[123]

MYPT1

Myosin-binding subunit of myosin phosphatase 1 (MYPT1) is the best characterized myosin light chain binding subunit (MBS). MYPT1 brings together the phosphatase catalytic subunit with its substrate and also plays a role in the regulation of phosphatase activity. MYPT1 can be phosphorylated by several kinases including ROCK1 and ROCK2, which inhibits phosphatase function. Beside MYPT1 there are four other proteins that may act as MBS (MYPT2, MYPT3, MBS85, TIMAP).[120]

Akt

The serine/threonine protein kinase Akt plays an important role in the maintenance of cellular processes including proliferation, cell growth, survival and metabolism. Furthermore Akt has been shown to regulate multiple processes that control invasive migration including cell motility and actin organization.[124,125]

2.2.8 PDGFR inhibitors

Imatinib mesylate (Glivec; Novartis) was specifically designed to interact with the ATP-binding site of tyrosine kinases. It has a high degree of specificity for the Abelson (ABL) kinases, PDGFR and c-KIT tyrosine kinases.[126] It has been shown that imatinib is an effective therapy for patients with CML (chronic myelogenous leukemia). As an ATP analogue, it competitively binds to the fusion BCR-ABL tyrosine kinase, which is the result from the oncogenic (9;22) chromosomal translocation.[127] It has also been shown that imatinib inhibits growth and proliferation in gastrointestinal stromal tumors (GIST) with c-kit mutations.[128] In patients with metastatic dermatofibrosarcoma protuberans (DFSP), which is caused by activation of PDGFRB, imatinib was shown to inhibit growth of the tumor through inhibiting PDGFRB tyrosine kinase activity.[129]

Recent studies suggest that imatinib may also directly influence immune cells such as T lymphocytes or dentritic cells. Stimulating as well as suppressive effects of imatinib have been reported.[130-132]

Other tyrosine kinase inhibitors, such as nilotinib (trade name Tasigna, Novartis), have been developed to overcome the problem of resistance to imatinib. Novel kinase inhibitors have stronger affinities to the ATP-binding sites of tyrosine kinases and thus are more potent compared to imatinib.[133]

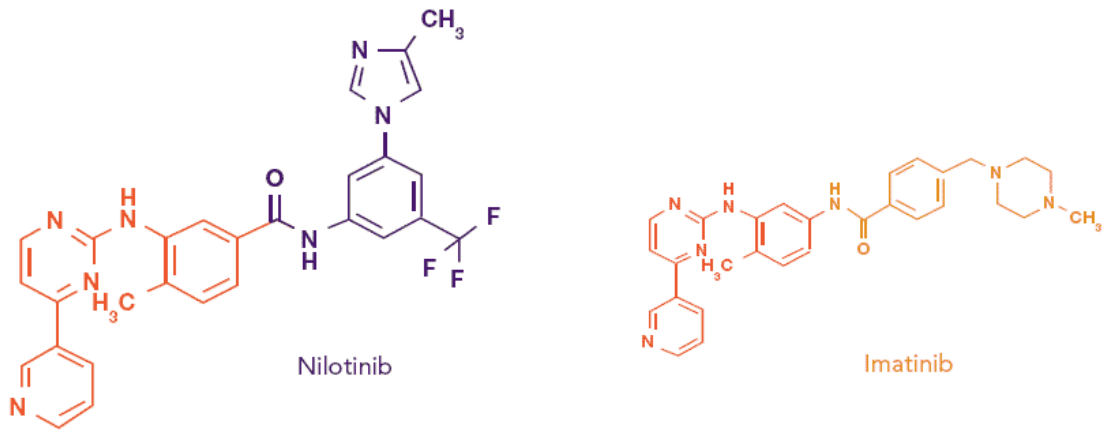

Figure 8. Chemical structure of nilotinib and imatinib. Taken from Weisberg et al., 2005

3 Aim

Imatinib treated *CD4*-NPM-ALK mice have a survival advantage and show reduced metastasis compared to untreated *CD4*-NPM-ALK mice.[134]

In imatinib-treated *CD4*-NPM-ALK-*CD4*$^{\Delta\Delta JUN}$ mice, no tumors developed during a 30-week observation period, and tumor cell dissemination to distant organs was blocked completely. Based on the data, we wanted to investigate the lymphomas regarding differences in stromal markers and tumor vasculature. Furthermore we wanted to elucidate whether there are differences in the expression of motility proteins, which play a role in the malignant behavior of tumor cells.

4 Materials and Methods

4.1 Solutions and Reagents

10x PBS

28.8 g Na_2HPO4

5.2 g NaH_2PO4

90 g NaCl

pH 7.2 – 7.6

ddH_2O to 1 liter

(10X PBS-T: 10x PBS + 0.1 % Tween-20)

10x TBS (0.5 M)

12.1 g Tris-Base

87.7 g NaCl

pH 7.5

ddH_2O to 1 liter

(10X TBS-T: 10x TBS + 0.1 % Tween-20)

50x TAE buffer

242 g Tris base

57.1 g acetic acid

100 ml 0.5 M EDTA (pH 8.0)

ddH_2O to 1 liter

DNA Extraction buffer

50 mM Tris-HCl pH8

100 mM NaCl

100 mM EDTA

1 % SDS

Lysis buffer

50 mM Tris-HCl ph 7.4

150 mM NaCl

5 mM EDTA

0.1 % Triton X-100

1x complete proteinase inhibitor cocktail (Roche, Basel, Switzerland)

1x HALT phosphatase inhibitor (Thermo Fisher Scientific, Waltham, USA)

ddH_2O

2x SDS loading buffer

126 mM Tris-HCL pH 6.8

100 mM DTT

4 % SDS

20 % Glycerin

0.02 % Bromphenolblue

ddH_2O

Electrophoresis buffer

3 g Tris

14.4 g Glycine

1 g SDS

ddH_2O to 1 liter

Transfer buffer

2.5 g Tris

11.2 g Glycine

200 ml Methanol

ddH_2O to 1 liter

Blocking solution

TBS-T

5 % milk powder

Agarose gel

2 g agarose

100 ml ddH_2O

2 µl Midori Green DNA stain

Gradient SDS polyacrylamide gels

	5 %	15 %	Stacking gel
1.5 M Tris pH 8.8	10 ml	10 ml	
1 M Tris pH 6.8			2.5 ml
30 % acrylamide mix	6.8 ml	20 ml	3.4 ml
10 % ammonium persulfate	0.4 ml	0.4 ml	0.2 ml
10 % SDS	0.4 ml	0.4 ml	0.2 ml
TEMED	2 µl (per gel)	1 µl (per gel)	20 µl per 20 ml
ddH_2O	22 ml	9.2 ml	13.6 ml

4.2 Cell lines

The cell lines CD4-417 and CD4-4, which were isolated from tumors of *CD4*-NPM-ALK mice [39], and the human ALCL cell line SR-786 were maintained in RPMI 1640 medium (Gibco, Invitrogen, Karlsruhe, Germany) supplemented with 10 % fetal bovine serum (Gibco, Invitrogen, Karlsruhe, Germany) and 1 % penicillin/streptomycin (Gibco, Invitrogen, Karlsruhe, Germany). The human chronic myelogenous cell line K562 was grown in DMEM (Gibco, Invitrogen, Karlsruhe, Germany) supplemented with 2 mM L-glutamine, 10 % fetal bovine serum (Gibco, Invitrogen, Karlsruhe, Germany) and 1 % penicillin/streptomycin (Gibco, Invitrogen, Karlsruhe, Germany). Cells were seeded at $5x10^5$ cells per ml culture medium and incubated at 37 °C in a humidified atmosphere containing 5 % CO_2.

4.3 Mice

Mice carrying the human NPM-ALK fusion gene expressed under the T-cell specific *CD4* promoter [39] were crossed with mice carrying loxP-flanked *JUN* [70] and/or *JUNB* [69], as well as with mice carrying *CD4*-Cre [71]. These intercrosses had the genetic background C57BL/6 × BALB/c. Mice were housed under specific pathogen-free (SPF) conditions and handled according to the ethical guidelines of the Medical University of Vienna. Mice that developed tumors were sacrificed and tumors were excised and weighed. One half of each tumor sample was snap-frozen in liquid nitrogen and stored at -80 °C. The other half, as well as spleen, lungs, kidneys and liver, were fixed with formalin and embedded in paraffin.

4.4 Genotyping

DNA extraction

Small ear pieces of 3 weeks old mice were cut and digested over night at 55 °C in 400 µl DNA extraction buffer and 0.25 mg/ml Proteinase K while shaking. Samples were mixed 5 min on an Eppendorf mixer. After addition of 250 µl 4M NaCl, samples were shortly mixed and centrifuged for 10 min at 13 000 rpm. Fluid without top phase or pellet was transferred into a new tube. After adding 400 µl isopropanol, the samples were mixed for 2 min and centrifuged at 13 000 rpm for 5 min. The pellets were washed with 70 % EtOH, air-dried and resuspended in 200 µl ddH2O. The DNA was incubated at 37 °C for 2 hours while shaking. DNA purity and concentration was measured using a with NanoDrop spectrophotometer (Thermo Scientific, Wilmington, USA).

PCR

Mice were genotyped for NPM-ALK, Cre, JUNB and JUN using following components for a single reaction: 1 µl genomic DNA, 12.5 µl GoTaq Green Master Mix (Promega, Madison, USA), 0.5 µl DMSO, 0.5 µl fwd Primer, 0.5 µl rev Primer, 10 µl ddH_2O.

Primers used:

ALK: Fwd: 5' TCC CTT GGG GGC TTT GAA ATA ACA CC 3'
Rev: 5' CGA GGT GCG GAG CTT GCT CAG C 3'
Cre: Fwd: 5' ATG CTT CTG TCC GTT TGC CG 3'
Rev: 5' TGA GTG AAC GAA CCT GGT CG 3'
JUN: Fwd: 5' CTC ATA CCA GTT CGC ACA GGC GGC 3'
Rev: 5' CCG CTA GCA CTC ACG TTG GTA GGC 3'
JUNB: Fwd: 5'GGG AAC TGA GGG AAG CCA CGC CGA GAA AGC 3'
Rev: 5' AGA GTC GTC GTG ATA GAA AGG 3'

Following program was used with a thermal cycler (Bio-Rad, Hercules, USA):

1. 94 °C for 10 minutes
2. 94 °C for 1 minute
3. 57 °C for 1 minute
4. 72 °C for 1 minute
5. 46 times steps 2-4
6. 72 °C for 10 minutes

Electrophoresis

Together with a 100 bp DNA ladder (Fermentas, Burlington, Canada), PCR products were separated on 2 % agarose gels (including Midori Green DNA Stain) in Tris-Acetate-EDTA (TAE) buffer solution at 120 V for 45 minutes. The gels were visualized using a UV transilluminator.

4.5 Imatinib treatment of CD4-NPM-ALK mice

CD4-NPM-ALK and *CD4*-NPM-ALK-*CD4*$^{\Delta\Delta JUN}$ mice received PBS or imatinib mesylate (0.1 mg / g bodyweight / per day) by oral gavage. Treatment started when mice were 6 weeks of age, cutoff was performed when mice reached 30 weeks of age. All animal experiments were approved by the ethical committee for animal experiments of the Medical University of Vienna and the Federal Ministry of Science and Research of Austria.

4.6 Xenograft experiment

Preparation of cells

The cell number of the cell line CD4-417 was determined using the CASY 1 cell counter (Schärfe-System, Reutlingen, Germany). Cells were washed two times with PBS and resuspended in fresh PBS.

Engraftment

$5x10^6$ cells were implanted subcutaneously into the right flanks of 12 week-old female SCID mice, which were obtained from Charles River (Wilmington, USA) and kept in Specific Pathogen-Free-facilities at the Ludwig Boltzmann Institute for Cancer Research, Vienna.

Preparation of imatinib/nilotinib

Imatinib mesylate and nilotinib tablets were dissolved in distilled water over night and subsequently sterilized by filtration.

Treatment

When tumors had grown to a size of approximately 0.5 cm in diameter, mice were separated into three groups. They received every day, for a period of ten days, either imatinib (200 mg per kilogram of body weight), nilotinib (200 mg per kilogram of body weight) or PBS by gavage. Tumor sizes were measured every day by means of a sliding caliper.

4.7 Immunohistochemistry

Preparation

Tumor samples were fixed in 4 % paraformaldehyde, and embedded in paraffin before being sectioned. Slides were incubated over night at 56 °C and de-paraffinzed and rehydrated using following series of washes: two xylene washes (10 min each), followed by two 100 % ethanol rinses (10 min each); followed subsequently by 95 %, 70 % and 50 % ethanol and two ddH_2O washes. To unmask the antigens, slides were treated with an antigen retrieval buffer (Tris-EDTA pH 9.0; sodium citrate pH 6.0) and heated using a microwave oven, a steam cooker or an autoclave. After cooling down for 30 minutes, slides were washed with PBS and then treated with 3 % hydrogen peroxidase to inactivate endogenous peroxidase. Slides were then subsequently treated with Avidin/Biotin Blocking Kit (Vector Laboratories, Burlingame, USA) and Universal Mouse HRP-Kit (IDLabs, London, USA) according to the manufactor´s protocol.

Labeling

The primary antibody was diluted to the appropriate concentration in 1 % BSA/PBS, applied to each section and incubated O/N at 4 °C in a humidified chamber. After washing with PBS, the sections were incubated with the appropriate secondary HRP-conjugated antibody (diluted in PBS) for one hour at room temperature. Sections were stained using DAB Substrate Kit (Abcam, Cambridge, UK) and counterstained with Hematoxylin.

Visualization

Immunohistochemical analysis was performed using Zeiss Axiomager Z1 microscope and Tissue Quest™ software (TissueGnostics GmbH, Vienna, Austria).

Primary antibodies

Anti-CD31 (1:50, DIA 310, Dianova, Hamburg, Germany)
Anti-S100A/B (1:500, Z0311, Dako, Glostrup, Denmark)
Anti–collagen IV (1:50, AB756P, Millipore, Billerica, USA)
Anti-alpha-smooth muscle actin (1:200, MS-113, Thermo Scientific, Fremont, USA)
Anti-vimentin (1:80, AB28028, Abcam, Cambridge, UK)

4.8 Western Blot

Protein extraction

Tumor samples were obtained from imatinib treated and untreated *CD4*-NPM-ALK and *CD4*-NPM-ALK-*CD4*$^{\Delta\Delta JUN}$ mice, frozen in liquid nitrogen and stored at -80 °C. Approximately 100 mg of tissue were homogenized and lysed with a dounce homogenizer in 1 ml lysis buffer. Samples were centrifuged for 15 min at 4°C (13000 rpm). The supernatants were transferred into new tubes; protein concentration was measured on NanoDrop spectrophotometer (Thermo Scientific, Wilmington, USA) at 280 nm.

Electrophoresis

After adding 2x SDS loading buffer, the samples were incubated at 95°C for 5 minutes and loaded onto a SDS polyacrylamide gradient gel (5 % - 15 %). PageRulerTMPrestained Protein ladder (Fermentas, Burlington, Canada) was used as a size marker. The proteins were electrophoresed at 130 V for 2 hours.

Transfer

The proteins were subsequently transferred onto a nitrocellulose membrane (poresize 0.2 µm Whatman Protran, GE healthcare, Buckinghamshire, UK) at 20 V over night.

Blocking

The membrane was dried and subsequently blocked in blocking solution for one hour at room temperature on a shaker.

Detection

The primary antibody was diluted in 5 % BSA/TBS-T and added to the membrane. After O/N incubation at 4 °C, the membrane was washed three times for 10 minutes with TBS-T and incubated with the second, peroxidase labeled, appropriate antibody (diluted in 5 % milk/TBS-T) for 1 hour at room temperature.

Analysis

After washing three times with TBS-T, the membrane was incubated with ECL Plus Western Blotting Detection Reagent (GE Healthcare, Buckinghamshire, UK) for a few minutes. Chemiluminescent signals were detected using Lumi-Imager F1 system (Boehringer, Mannheim, Germany) and quantified using LumiAnalyst software (Boehringer, Mannheim, Germany).

Primary antibodies

Anti-pERK (1:1000, #9106, Cell Signaling, Danvers, USA)
Anti-ERK (1:1000, #4695, Cell Signaling, Danvers, USA)
Anti-pMLC2 (1:500, #3671, Cell Signaling, Danvers, USA)
Anti-MLC2 (1:500, #3672, Cell Signaling, Danvers, USA)
Anti-pAKT (Ser473) (1:1000, #4058, Cell Signaling, Danvers, USA)
Anti-pAKT (Thr308) (1:1000, #9275, Cell Signaling, Danvers, USA)
Anti-ROCK1 (1:1000, #4035, Cell Signaling, Danvers, USA)
Anti-pMYPT1 (1:500, ABS45, Millipore, Billerica, USA)
Anti-MYPT1 (1:500, #2634, Cell Signaling, Danvers, USA)
Anti-ARP2/3 (1:1000, ab77084, Abcam, Cambridge, UK)
Anti-Paxillin (1:1000, sc-5574, Santa Cruz, Dallas, USA)
Anti-alpha Tubulin (1:7000, ab4074, Abcam, Cambridge, UK)

Secondary antibodies

Polyclonal rabbit anti-mouse IgG (HRP) (1:5000, R0207, Dako, Glostrup, Denmark);
Goat F(ab')$_2$ anti-rabbit IgG (H+L) (1:5000, L43000, Invitrogen, Camarillo, USA)

4.9 Dose-response assay

Cell number was measured using the CASY 1 cell counter (Schärfe System, Reutlingen, Germany). 25000 cells per well were seeded in 100 µl of the appropriate medium. A 10 mM stock of imatinib mesylate (Novartis, Basel, Switzerland) was prepared: the tablet was dissolved in distilled water over night and subsequently sterilized by filtration. Imatinib was added to cells in concentrations from 0.01 µM to 30 µM on the first day and again after 48 hours. After 72 hours of incubation at 37 °C, cell viability was determined using CellTiter 96® Aqueous Non-Radioactive Cell Proliferation Kit (Promega, Fitchburg, USA). The assay is based on a colorimetric reaction in which a tetrazolium compound is bioreduced by cells into a formazan product. The absorbance at 490 nm was recorded using an ELISA plate reader (BioTek, Winooski, USA).

For data interpretation the background absorbance was subtracted from all data points. IC_{50} values were calculated with GraphPad Prism software using the sigmoidal dose-response function.

5 Results

5.1 Response of NPM-ALK cell lines to imatinib

Two NPM-ALK cell lines (CD4-417, CD4-4), which derived from tumors of *CD4*-NPM-ALK mice [39], were tested for their response to the tyrosine kinase inhibitor imatinib. They were treated with different concentrations of imatinib (0.01 µM to 30 µM) and determined for viable cells by using CellTiter 96® Aqueous Non-Radioactive Cell Proliferation Kit (Promega, Fitchburg, USA). The human CML cell line K562, which expresses the abnormal fusion protein BCR-ABL and is known to be sensitive to imatinib at nanomolar concentrations, was taken for positive control. The human ALCL cell line SR-786, which neither expresses PDGFR nor BCR-ABL, served as negative control.
Imatinib concentrations from 0.01 µM to 30 µM were added in triplicate wells on the first day and again after 48 hours. The absorbance at 490 nm was recorded after 72 hours using an ELISA plate reader.

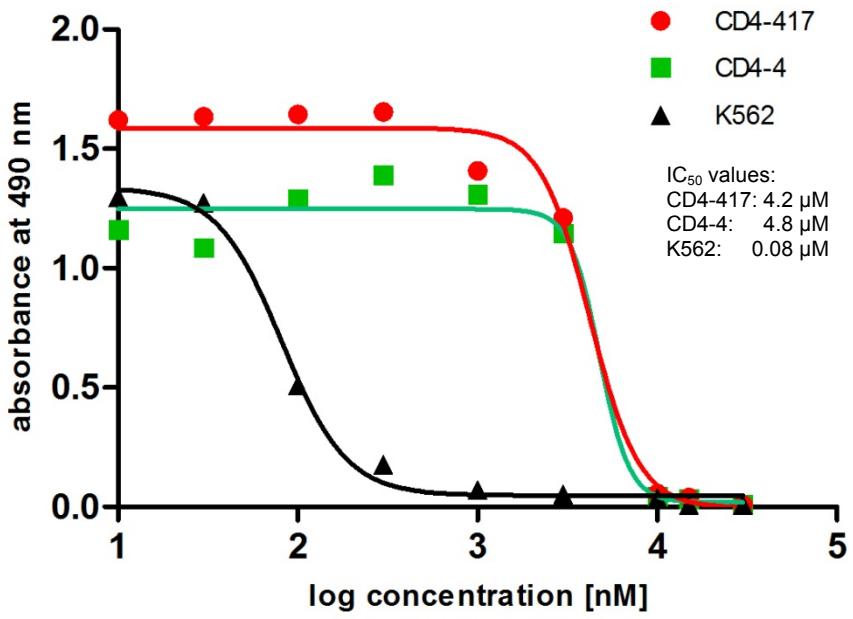

Figure 9. Imatinib dose response curve of mouse *CD4*-NPM-ALK cell lines. Cells were cultured with escalating concentrations of imatinib for 72 hours. The cell line K562 was taken for positive control. Cell viability was monitored by using MTS colorimetric assay. The data represent means of triplicate determinations.

Imatinib mesylate induced 50 % growth inhibition in mouse NPM-ALK cell lines CD4-4 and CD4-417 at concentrations that were 5 – 6 times higher than the IC_{50} for the positive control, cell line K562 (Fig 9). Viability of K562 cells decreased markedly when treated with an imatinib concentration above 0.03 μM and was extinguished in wells containing imatinib greater than 1 μM. Viability of the cell lines CD4-4 and CD4-417 diminished rapidly from an imatinib concentration of 3 μM, reaching 0% viability at 10 μM drug concentration. The negative control, cell line SR-786 (data not shown), did not respond to imatinib at all. The calculated IC_{50} values for imatinib in the cell lines K562, CD4-417 and CD4-4 are 0.08 μM, 4.2 μM and 4.8 μM, respectively.

5.2 *Effect of imatinib and nilotinib on xenografted NPM-ALK tumors*

To investigate the effects of the tyrosine kinase inhibitors in vivo, CD4-417 cells, derived from a *CD4*-NPM-ALK mouse tumor [39], were injected into the flanks of 12 week old SCID mice. Solid tumors developed approximately two weeks after injection. Mice were separated into three groups of six mice each, and received for a period of ten days imatinib, nilotinib or PBS.

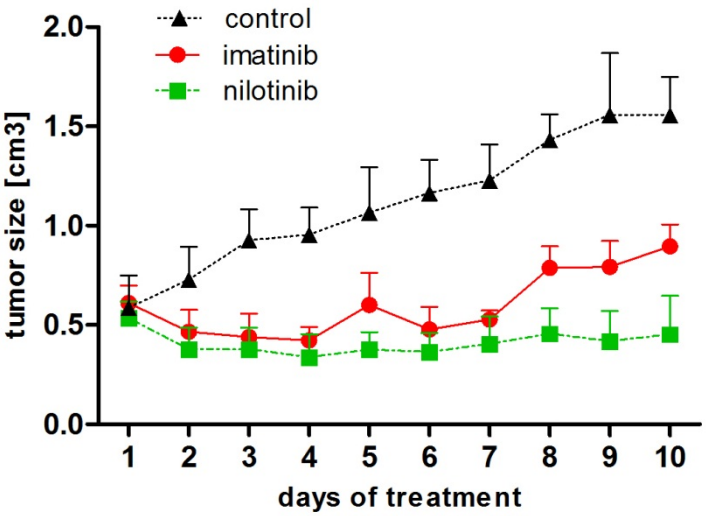

Figure 10. Tumor growth kinetics of mice that were engrafted with the NPM-ALK cell line CD4-417 and treated with imatinib, nilotinib or PBS. Six mice were taken for each group; the tumor sizes were measured every day over a period of 10 days. Error bars present

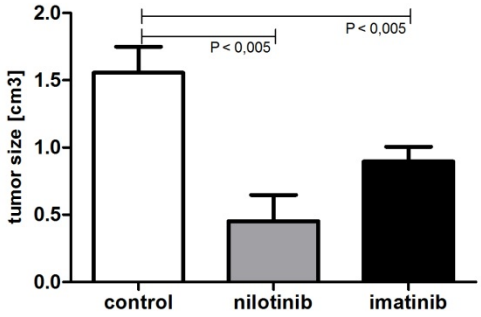

Figure 11. Tumor size on day 10 of treatment. The diagram shows the tumor size of each group measured on day 10 (after sacrificing). Error bars present s.d.

After a course of ten days, imatinib and nilotinib treated mice showed significantly reduced tumor sizes in contrast to the PBS controls (Fig. 11). At the beginning of the treatment, all tumors had approximately the same size – between 0.5 cm^3 and 0.6 cm^3. Mice that received PBS showed a steady increase in tumor volume over the period of 10 days. The average tumor size of this group on day 10 was 1.6 cm^3. Mice that were treated with imatinib showed a slightly increase in tumor size, but compared to controls, the volume was significantly reduced on day 10 (0.9 cm^3). The tumors of nilotinib treated mice slightly decreased in size – from the average size of 0.6 cm^3 on the first day of treatment to 0.5 cm^3 on day 10. Compared to controls, both drugs significantly reduced tumor volumes of transplanted *CD4*-NPM-ALK tumors within ten days treatment.

5.3 *Immunohistochemical analysis of microvessels and tumor stroma markers in imatinib-treated and untreated CD4-NPM-ALK and CD4-NPM-ALK-CD4$^{\Delta\Delta JUN}$ tumors*

Laimer et al.[22] showed that treatment with imatinib significantly increases survival time for *CD4*-NPM-ALK mice, which normally develop lymphomas within 15-20 weeks of age. However, imatinib treated *CD4*-NPM-ALK-*CD4*$^{\Delta\Delta JUN}$ mice did not develop tumors during a 30-week observation period. It was shown that pPDGFRB expression was completely reduced in imatinib treated *CD4*-NPM-ALK mouse lymphomas in contrast to untreated *CD4*-NPM-ALK lymphomas. In *CD4*-NPM-ALK-*CD4*$^{\Delta\Delta JUN}$ mice pPDGFRB expression was restricted to a few stroma cells.

Since PDGFRB signaling plays an important role in tumor angiogenesis and tumor stroma development, we wanted to investigate if the blockage of PDGFRB in imatinib treated mice would have an effect on tumor stroma and tumor microvessels. We used frozen tumor samples from *CD4*-NPM-ALK and *CD4*-NPM-ALK-*CD4*$^{\Delta\Delta JUN}$ mice that have been treated with imatinib or PBS and performed immunohistochemical stainings with five different markers (Fig.12 – 21).

CD31 is expressed constitutively on the surface of endothelial cells and is therefore a good marker to evaluate the degree of tumor angiogenesis.[135] Compared to *CD4*-NPM-ALK lymphomas, microvessel density was reduced in *CD4*-NPM-ALK-*CD4*$^{\Delta\Delta JUN}$ lymphomas. Sections of imatinib treated lymphoma samples displayed a lower microvessel density compared to untreated samples.

Alpha smooth muscle actin (alpha-SMA) is commonly used as a marker for myofibroblast formation.[136] Myofibroblasts arise from fibroblasts as part of stromal changes induced by cancer cells through paracrine and autocrine effects.[94] Expression of alpha-SMA was found to be significantly higher in untreated NPM-ALK lymphomas compared to knockout samples and imatinib treated lymphomas.

Collagen IV is a major component of basement membranes and provides structural support for the ECM. We used anti-collagen IV to compare the ECM extent of our lymphoma samples. The expression of collagen IV was severely reduced in *CD4*-NPM-ALK-*CD4*$^{\Delta\Delta JUN}$ lymphomas compared to *CD4*-NPM-ALK lymphomas. The expression was nearly at the same level in knockout tumors and treated lymphomas. The lowest expression of collagen IV was found in imatinib treated *CD4*-NPM-ALK-*CD4*$^{\Delta\Delta JUN}$ lymphomas.

Vimentin is a major cytoskeletal component of mesenchymal cells and is often used as marker of mesenchymal-derived cells during metastatic progression.[137,138]

S100 proteins are a large multi-gene family of proteins that are characterized by two EF-hand calcium-binding domains. They are involved in the regulation of cellular processes, including cell cycle regulation, cell growth and migration and cytoskeletal interactions.[139,140]

The expression of S100 proteins is often altered in tumors.[141] S100A2 is up-regulated in non-small cell carcinoma, associated with higher propensity of metastasis.[142] S100A4 is highly expressed in many tumors and its expression is a predictor of patient survival and metastasis. It was shown that S100A4 contributes to the metastatic process including invasion, migration and angiogenesis.[143] Beside others, S100A4 is a marker of the mesenchymal phenotype.[144] S100A11 expression is associated with advanced disease in prostate cancer [145] and it was shown to be up-regulated in anaplastic large cell lymphomas.[146]

CD4-NPM-ALK lymphomas showed significantly higher expression of vimentin and S100A/B compared to *CD4*-NPM-ALK-$CD4^{\Delta\Delta JUN}$ lymphomas. A severely reduced expression of the proteins was found in imatinib treated samples of *CD4*-NPM-ALK-$CD4^{\Delta\Delta JUN}$, compared to untreated samples.

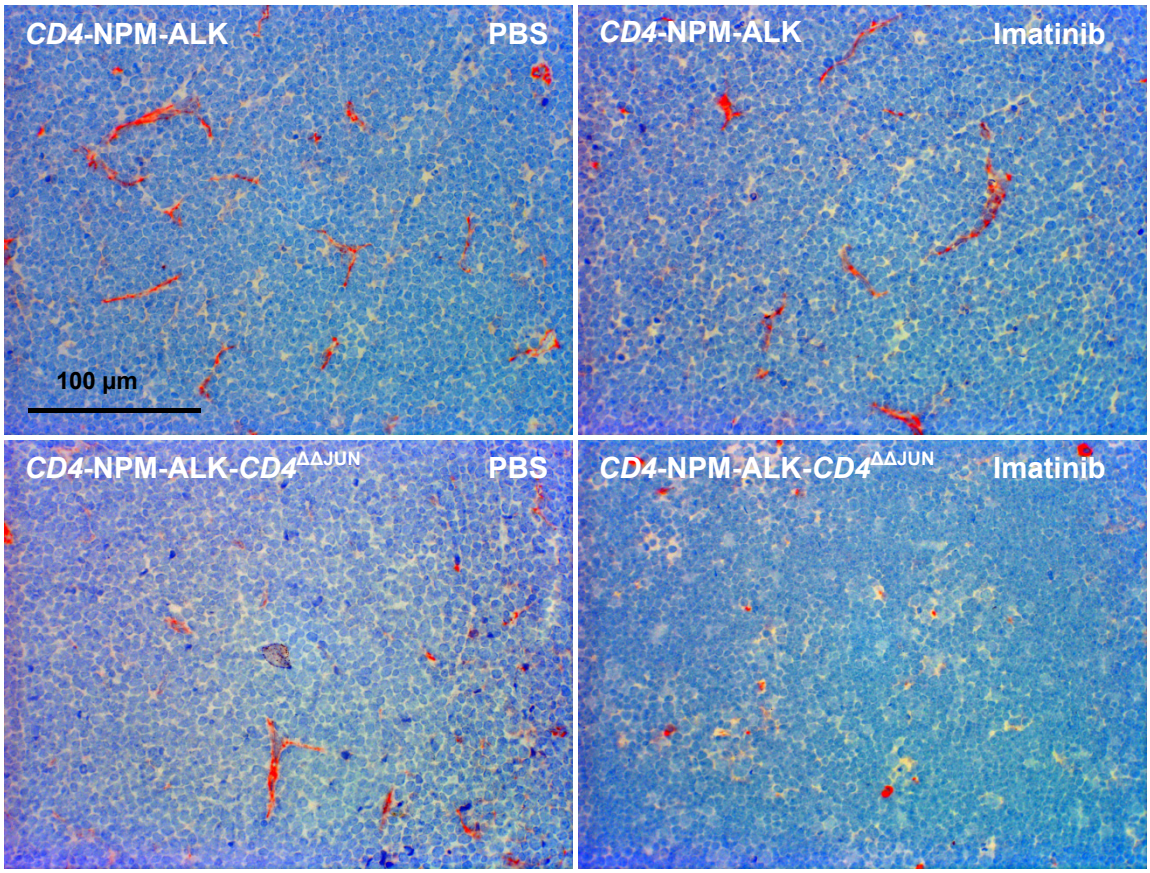

Figure 12. Immunohistochemical staining with anti-CD31 antibody. For each group – *CD4*-NPM-ALK mice treated and untreated, *CD4*-NPM-ALK-*CD4*$^{\Delta\Delta JUN}$ *mice* treated and untreated – one representative picture is shown.

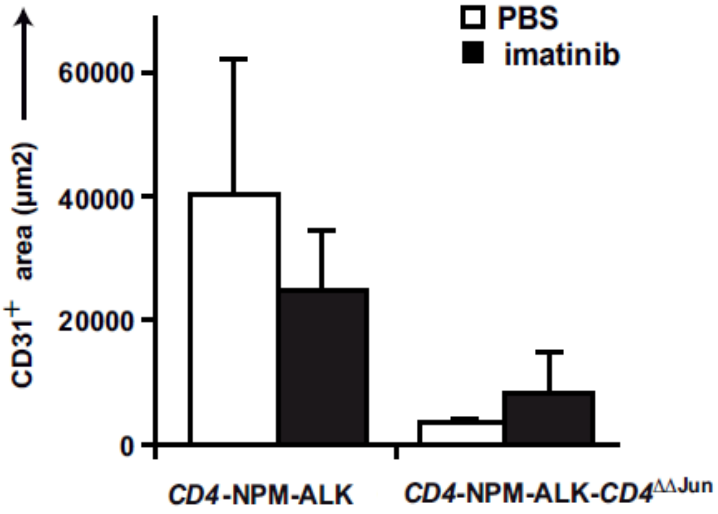

Figure 13. Analysis of CD31-staining. Three mice per group were analyzed; the numbers of positively stained areas per group were measured with TissueQuest^{TM} software and shown in bar graphs. Error bars represent s.d.

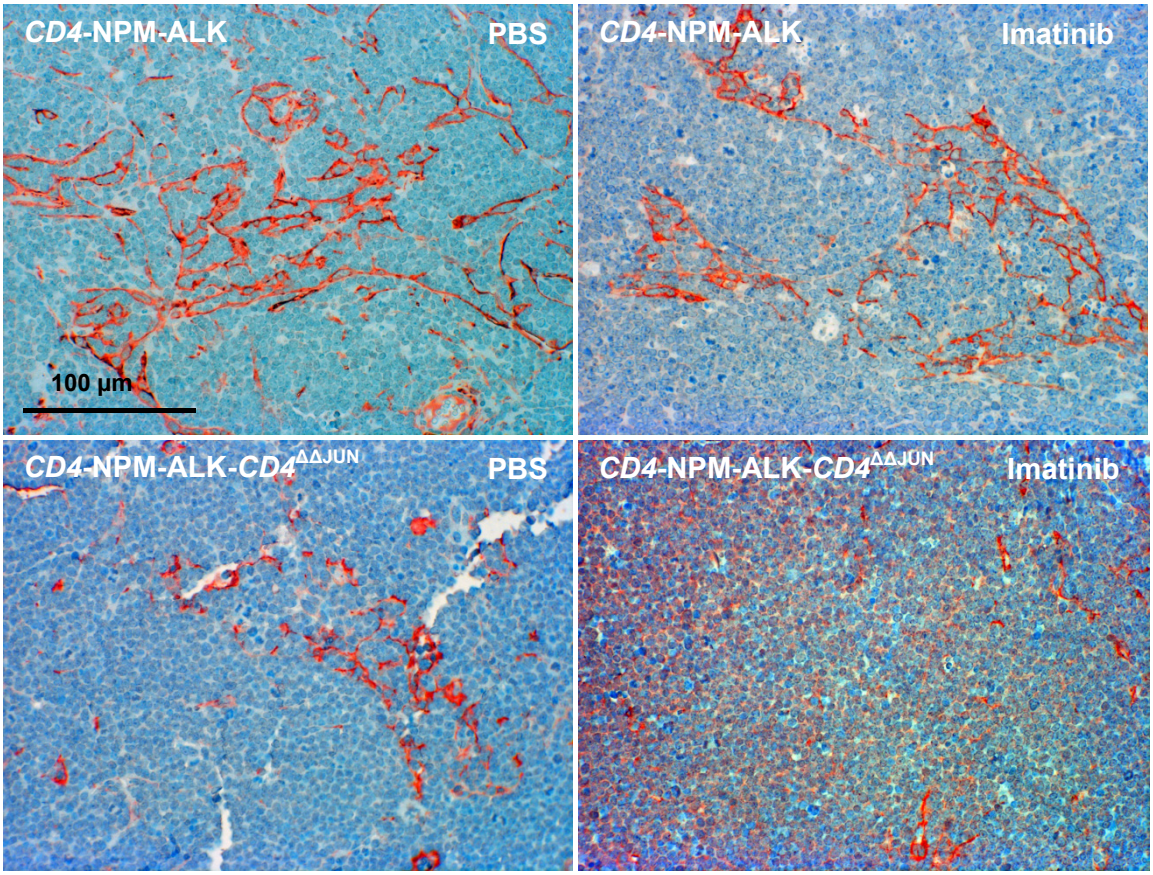

Figure 14. Immunohistochemical staining with anti-alpha-SMA antibody. For each group – *CD4*-NPM-ALK mice treated and untreated, *CD4*-NPM-ALK-*CD4*$^{\Delta\Delta JUN}$ mice treated and untreated – one representative picture is shown.

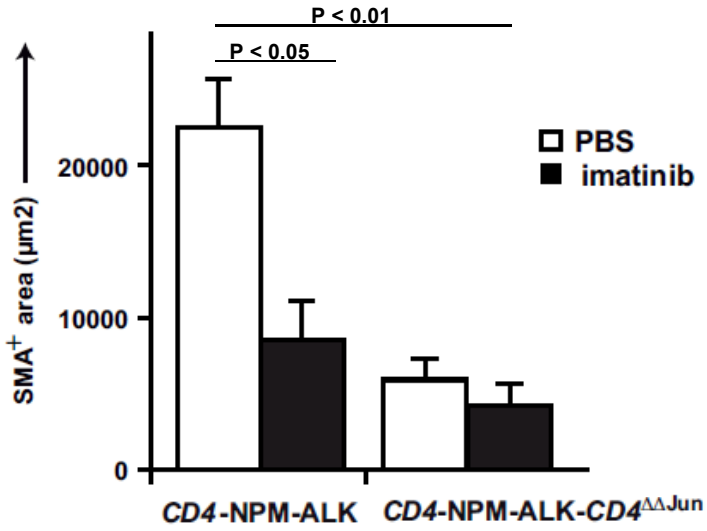

Figure 15. Analysis of alpha-SMA-staining. Three mice per group were analyzed; the numbers of positively stained areas per group were measured with TissueQuest^{TM} software and shown in bar graphs. Error bars represent s.d.

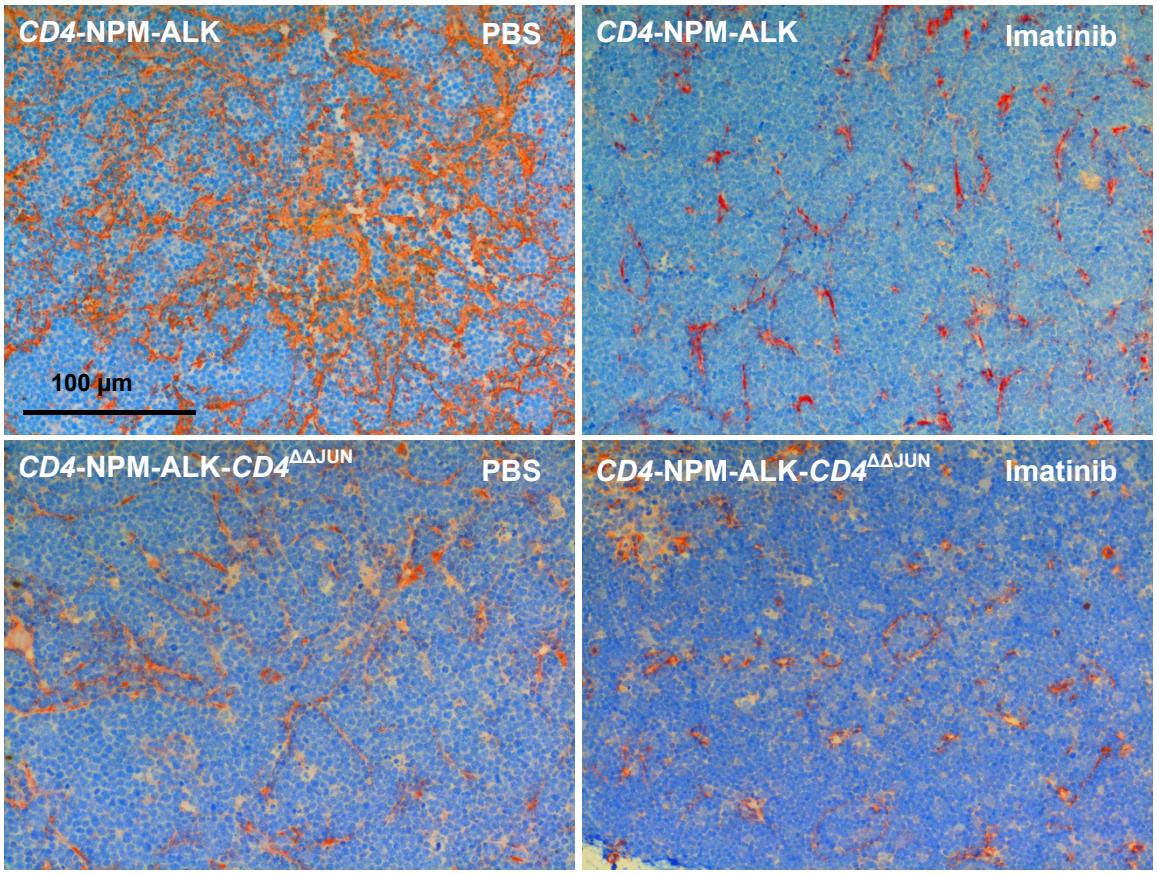

Figure 16. Immunohistochemical staining with anti-collagen IV antibody. For each group – *CD4*-NPM-ALK mice treated and untreated, *CD4*-NPM-ALK-*CD4*$^{\Delta\Delta JUN}$ mice treated and untreated – one representative picture is shown.

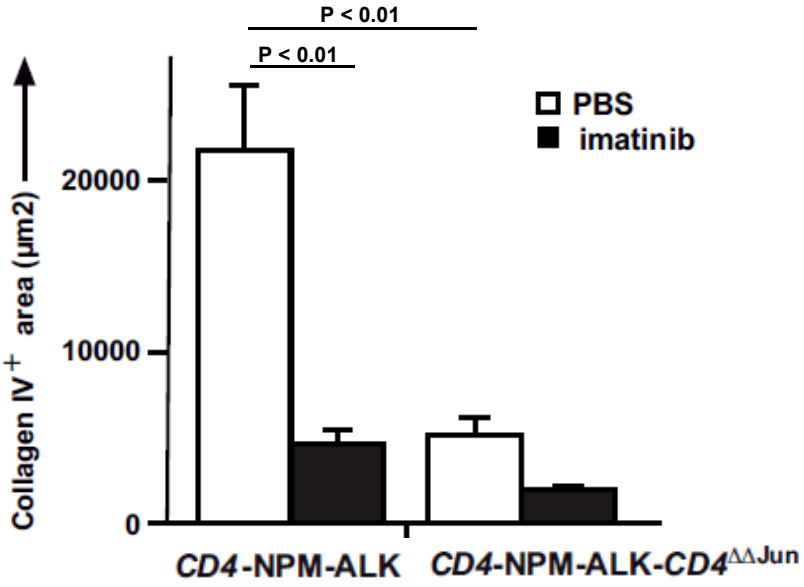

Figure 17. Analysis of collagen-IV-staining. Three mice per group were analyzed; the numbers of positively stained areas per group were measured with TissueQuest^{TM} software and shown in bar graphs. Error bars represent s.d.

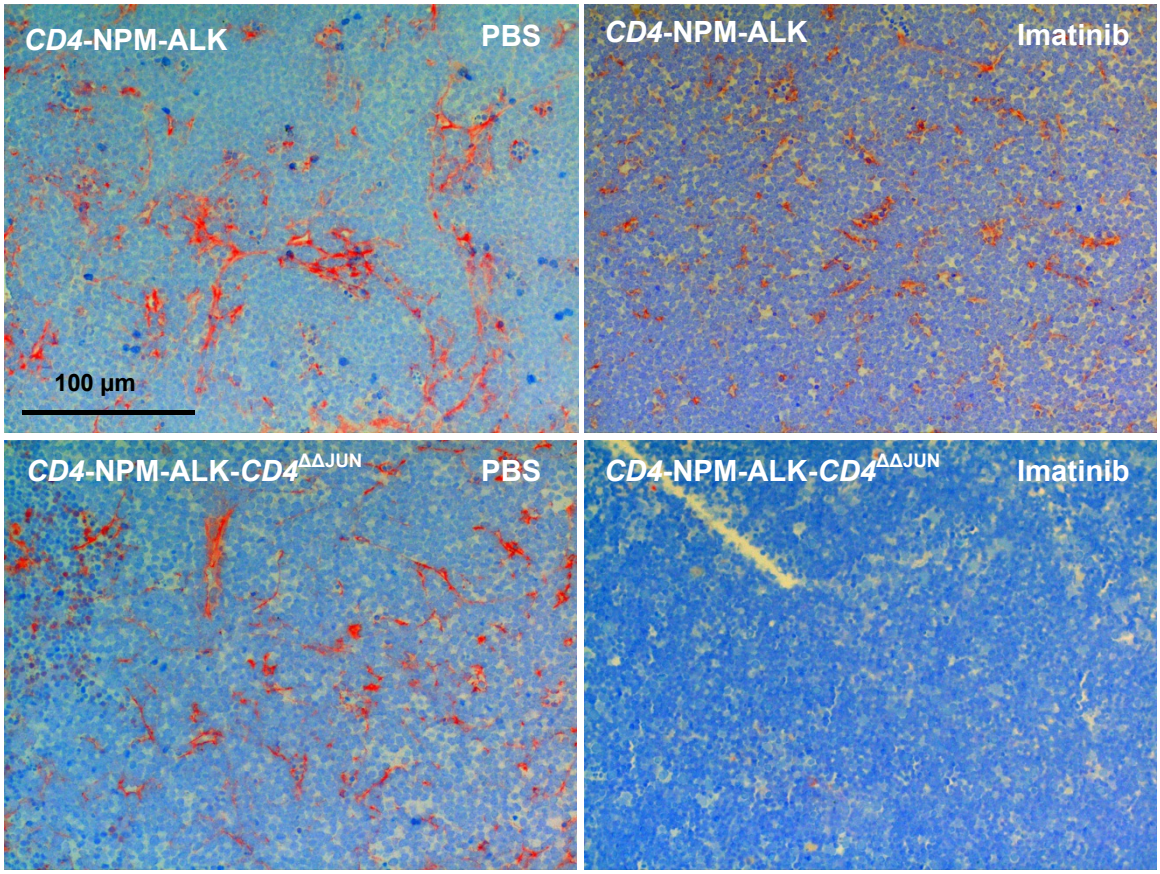

Figure 18. Immunohistochemical staining with anti-vimentin antibody. For each group – *CD4*-NPM-ALK mice treated and untreated, *CD4*-NPM-ALK-*CD4*$^{\Delta\Delta JUN}$ mice treated and untreated – one representative picture is shown.

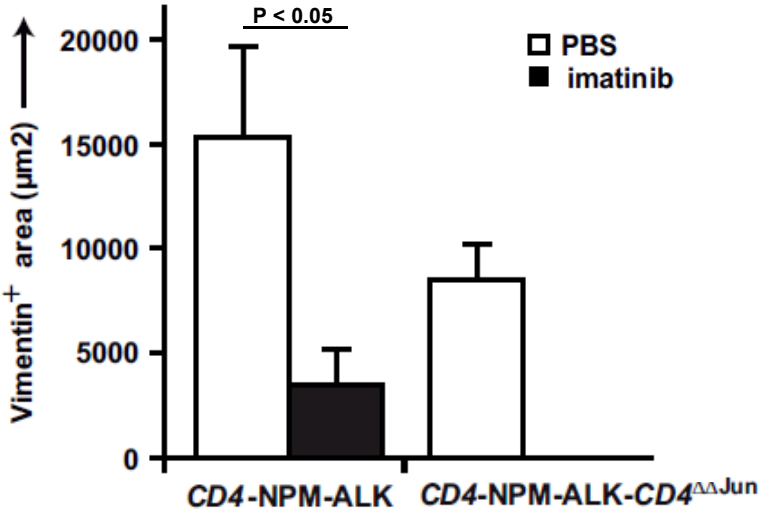

Figure 19. Analysis of vimentin-staining. Three mice per group were analyzed; the numbers of positively stained areas per group were measured with TissueQuest^{TM} software and shown in bar graphs. Error bars represent s.d.

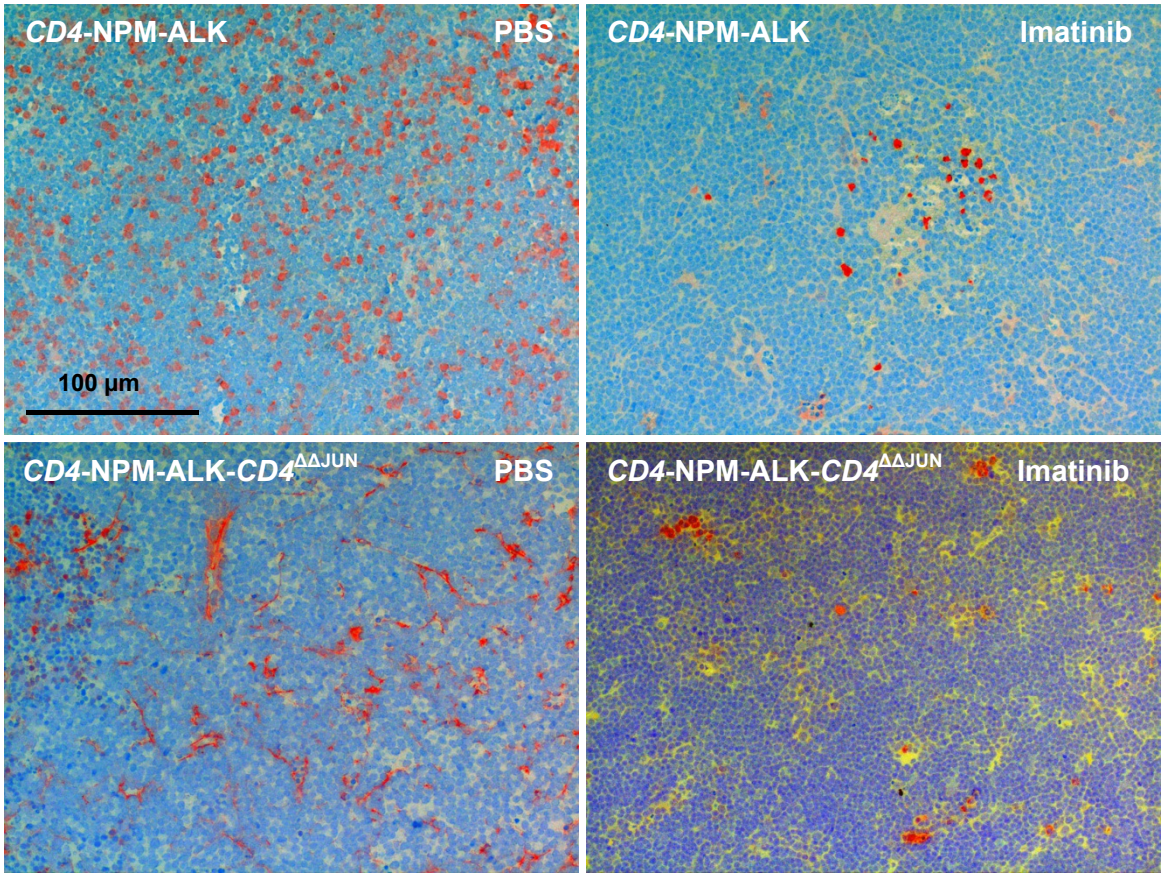

Figure 20. Immunohistochemical staining with anti-S100A/B antibody. For each group – *CD4*-NPM-ALK mice treated and untreated, *CD4*-NPM-ALK-*CD4*$^{\Delta\Delta JUN}$ mice treated and untreated – one representative picture is shown.

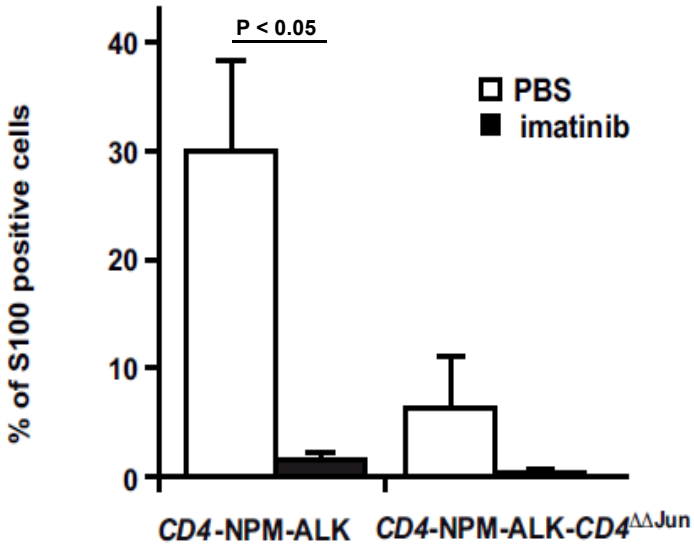

Figure 21. Analysis of S100A/B-staining. Three mice per group were analyzed; the numbers of positively stained areas per group were measured with TissueQuest^{TM} software and shown in bar graphs. Error bars represent s.d.

5.4 Expression of motility proteins in imatinib-treated and untreated CD4-NPM-ALK tumors and CD4-NPM-ALK-$CD4^{\Delta\Delta JUN}$ tumors

CD4-NPM-ALK lymphomas show aggressive invasion of NPM-ALK positive lymphoma cells into the livers of transgenic mice in contrast to *CD4*-NPM-ALK-$CD4^{\Delta\Delta JUN}$ lymphomas. In imatinib treated *CD4*-NPM-ALK-$CD4^{\Delta\Delta JUN}$ mice tumor cell dissemination to distant organs is completely blocked.[22]

To metastasize from the primary tumor site to distant organs, lymphoma cells must acquire a mobile phenotype.[109] The behaviour of lymphoma cells is probably based on mechanisms of migration of normal lymphocytes. To determine the expression of motility proteins in imatinib treated and untreated *CD4*-NPM-ALK lymphomas and *CD4*-NPM-ALK-$CD4^{\Delta\Delta Jun}$ lymphomas, we performed western blot analysis. The results are shown in Fig. 22-24.

Compared to *CD4*-NPM-ALK lymphomas, activation of ERK1/2 (pERK1/2) is significantly increased in *CD4*-NPM-ALK-$CD4^{\Delta\Delta JUN}$ lymphomas, whereas the expression of ERK1/2 is significantly reduced in these tumors. Treatment with imatinib does not seem to have an impact on pERK or ERK expression.

In two of three tested *CD4*-NPM-ALK-$CD4^{\Delta\Delta JUN}$ tumors, expression of pMLC2 and MLC2 is increased compared to *CD4*-NPM-ALK tumors. In imatinib treated and untreated lymphomas, expression of pMLC2 and MLC2 is nearly at the same level.

Expression of MYPT1 seems to be reduced in imatinib treated lymphomas, whereas the phosphorylated form of MYPT1 is at the lowest level in *CD4*-NPM-ALK-$CD4^{\Delta\Delta JUN}$ samples.

ARP2/3 expression is significantly reduced in *CD4*-NPM-ALK-$CD4^{\Delta\Delta JUN}$ lymphomas compared to untreated *CD4*-NPM-ALK lymphomas. Treated lymphomas show a slightly reduced ARP2/3 expression compared to untreated samples.

Expression of ROCK1 and Paxillin seems to be elevated in untreated *CD4*-NPM-ALK lymphomas, compared to imatinib treated samples. Both factors have their lowest expression levels in *CD4*-NPM-ALK-$CD4^{\Delta\Delta JUN}$ tumors.

P(Ser472)Akt and p(Thr308)Akt have similar expression levels. Both show elevated expression levels in *CD4*-NPM-ALK-$CD4^{\Delta\Delta JUN}$ lymphomas and reduced levels in untreated *CD4*-NPM-ALK lymphomas.

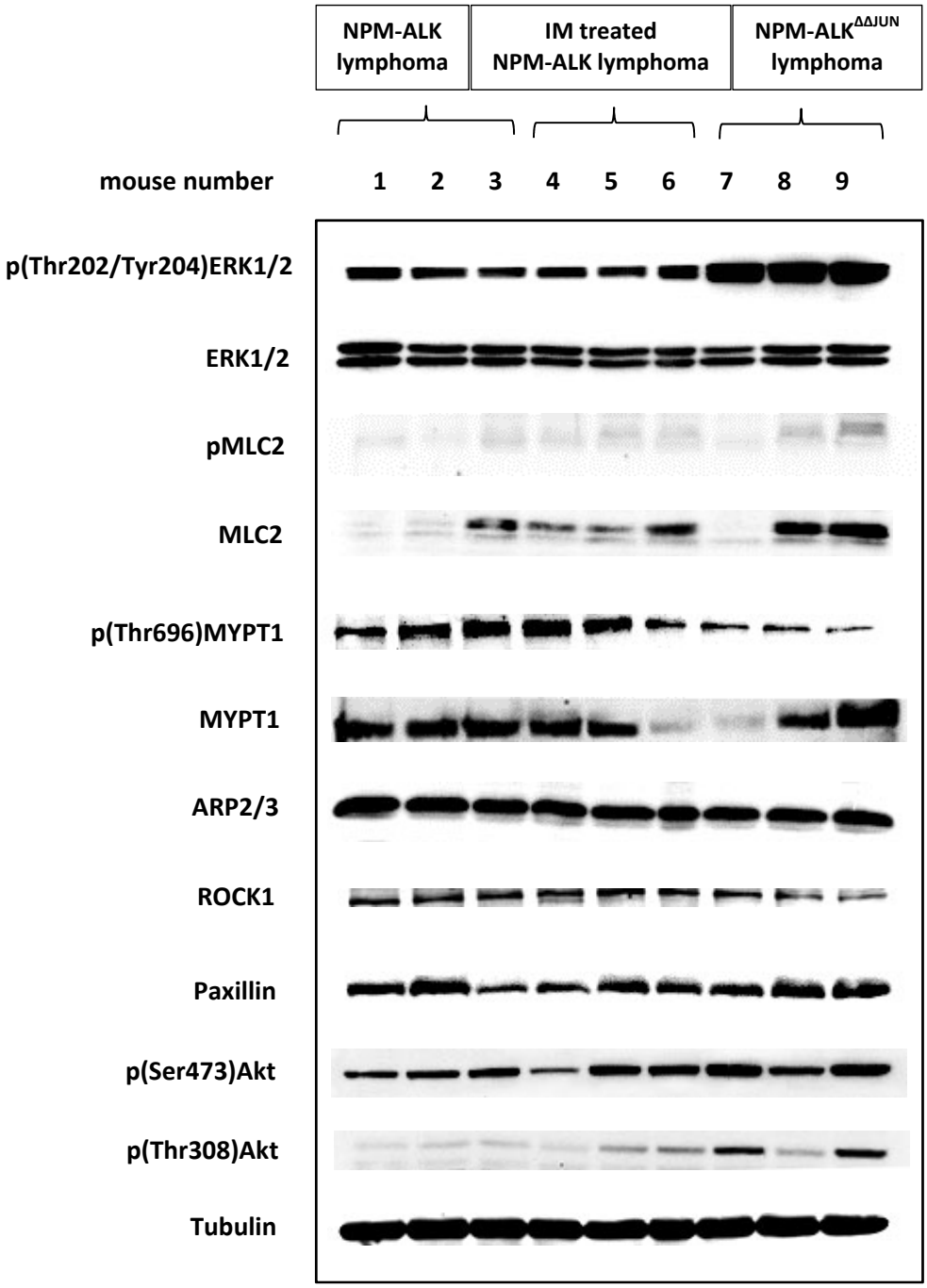

Figure 22. Western Blot analysis of motility proteins in imatinib treated and untreated *CD4*-NPM-ALK lymphomas and *CD4*-NPM-ALK-*CD4*$^{\Delta\Delta JUN}$ lymphomas. Chemiluminescent signals were imaged with the Lumi-Imager F1 system (Boehringer, Mannheim, Germany).

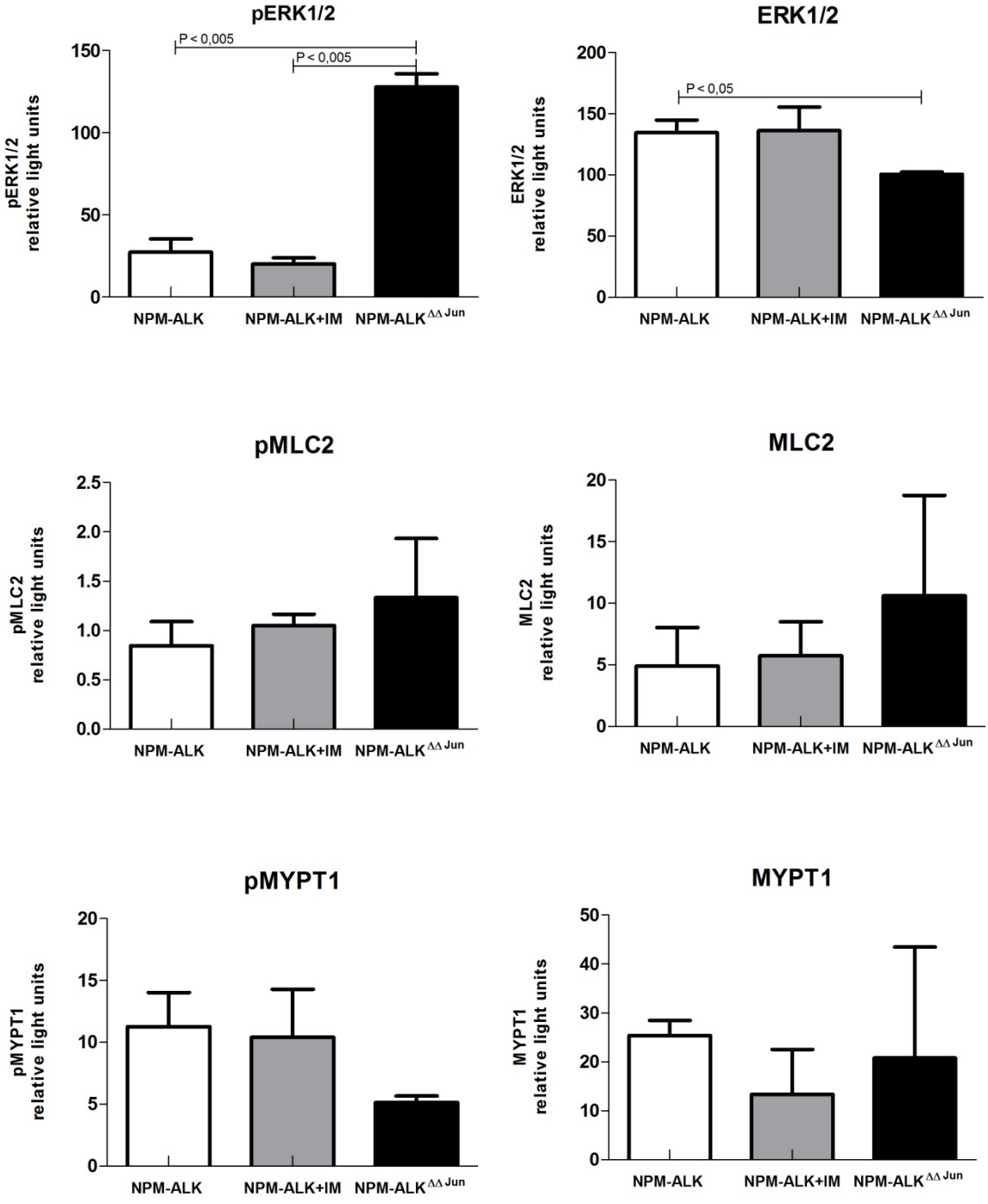

Figure 23. Quantification of western blots. pERK1/2, pERK, pMLC2, MLC2, pMYPT1 and MYPT1 expression in imatinib treated and untreated *CD4*-NPM-ALK lymphomas and *CD4*-NPM-ALK-*CD4*$^{\Delta\Delta JUN}$ lymphomas. Maximal luminescence intensities were measured as BLUs (Boehringer light units) with the LumiAnalyst software (Boehringer, Mannheim, Germany). Mean ± SD; normalized to the loading control tubulin.

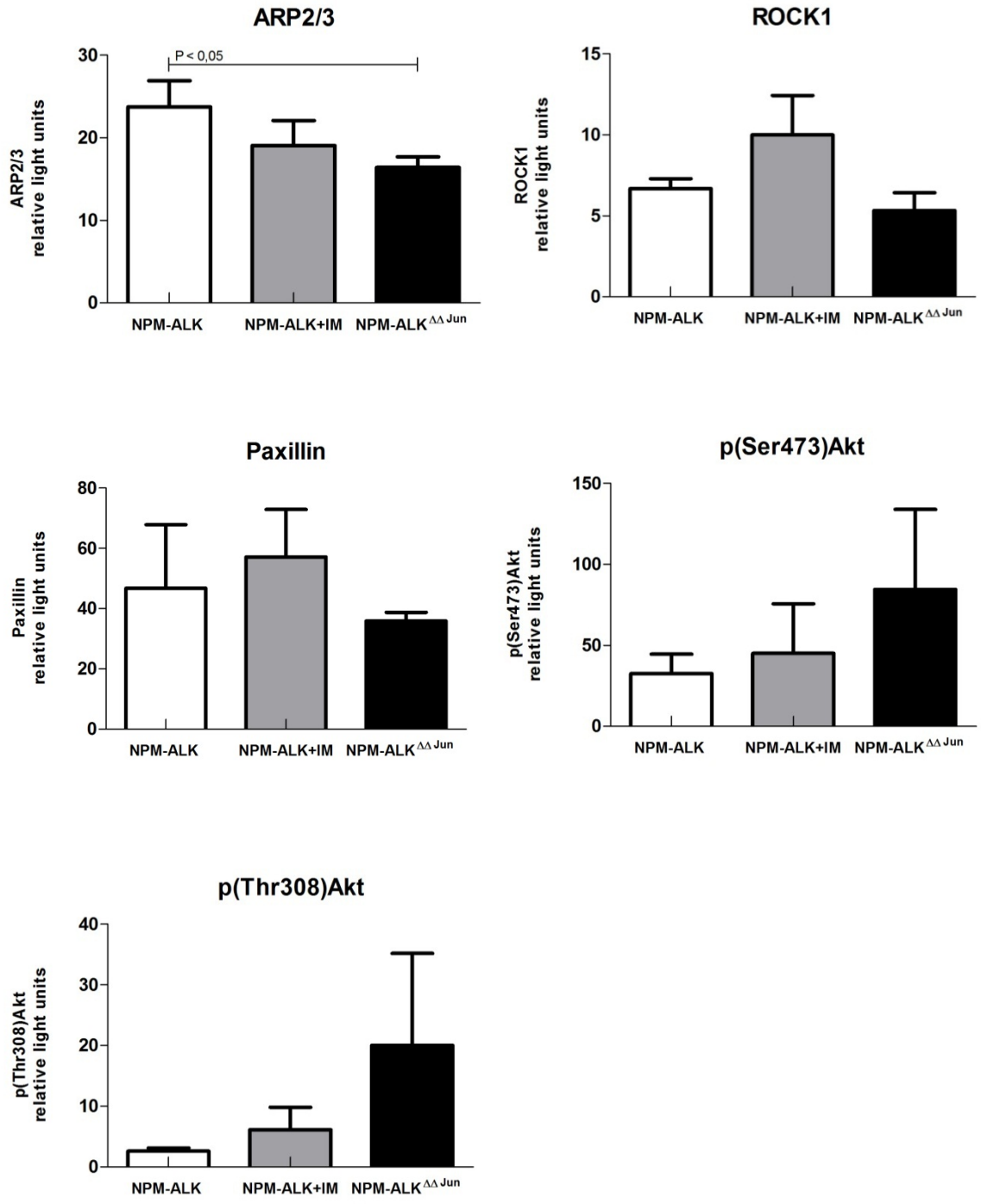

Figure 24. Quantification of western blots. ARP2/3, ROCK1, Paxillin, p(Ser473)Akt and p(Thr308)Akt expression in imatinib treated and untreated *CD4*-NPM-ALK lymphomas and *CD4*-NPM-ALK-*CD4*$^{\Delta\Delta JUN}$ lymphomas. Maximal luminescence intensities were measured as BLUs (Boehringer light units) with the LumiAnalyst software (Boehringer, Mannheim, Germany). Mean ± SD; normalized to loading control.

6 Discussion

The fusion protein NPM-ALK is the most common chromosomal aberration in anaplastic large cell lymphomas (ALCL). It harbors a constitutively active tyrosine kinase that activates many signaling cascades. Together with the RAS-MAPK pathway, the JNK MAPK pathway promotes actions of downstream transcription factors, such as AP-1.[55,57] High expression of JUN and JUNB is a hallmark feature of ALK^+ ALCL.[36,54,56] The factors initiate the transcription of growth promoting proteins and regulators of apoptosis and play a role in tumor invasion.[45] In a transgenic *CD4*-NPM-ALK mouse model,[39] *CD4*-Cre-mediated knockout of *JUN* and *JUNB* lead to significant delay in tumor onset. It could be shown that PDGFRB expression was reduced in *CD4*-NPM-ALK-$CD4^{\Delta\Delta JUN}$ lymphomas, which lack JUN/JUNB expression, compared to *CD4*-NPM-ALK lymphomas. PDGFRB was shown to be directly regulated by JUN and JUNB.[22]

Since indirect blockage of PDGFRB expression by knockout of JUN and JUNB lead to significant survival advantage of NPM-ALK mice, we wanted to investigate, if direct blockage of PDGFRB by tyrosine kinase inhibitors would have similar effects. The first step was to examine the mouse NPM-ALK cell lines CD4-4 and CD4-417 for their response to the tyrosine kinase inhibitor imatinib mesylate. The human CML cell line K562 was taken as a positive control. It harbors the fusion protein BCR-ABL [147], which is seen as the molecular hallmark of chronic myeloid leukemia (CML) and presumably as the cause of its development. Imatinib mesylate was developed as a potent and specific inhibitor of ABL tyrosine kinase.[148] Imatinib mesylate was shown to induce growth arrest and apoptosis in the human CML cell line K562.[149]

The calculated IC_{50} values for the *CD4*-NPM-ALK cell lines were 5 – 6 times higher than the value for K562, indicating that the effect of growth inhibition is limited in *CD4*-NPM-ALK cell lines compared to the highly sensitive CML cell line. But in contrast to the negative control, human ALCL cell line SR-786, which expresses NPM-ALK but not the PDGFRB, the mouse cell lines responded to imatinib concentrations greater than 1 µM.

Next we investigated the blockage of PDGFRB by tyrosine kinases in vivo. SCID mice were transplanted subcutaneously with the mouse NPM-ALK cell line CD4-417. Mice that have been treated for ten days with imatinib or nilotinib showed a significantly reduced tumor growth compared to controls. According to literature nilotinib is thought to display similar specificity towards PDGFRB [150], but our data suggest a stronger effect of NPM-ALK tumor growth inhibition by the tyrosine kinase inhibitor nilotinib compared to imatinib.

The effect of PDGFRB blockage by tyrosine kinase inhibitors in vivo (significantly reduced tumor growth) was much stronger than we had expected. Although NPM-ALK cell lines did respond to imatinib, the IC_{50} values were relatively high. Therefore we assumed an additional effect of PDGFRB inhibition in NPM-ALK tumors, probably blockage of PDGFRB signaling in the tumor stroma. A second reason to investigate the tumor stroma was the fact that in contrast to *CD4*-NPM-ALK mice, *CD4*-NPM-ALK-*CD4*$^{\Delta\Delta JUN}$ mice and imatinib treated *CD4*-NPM-ALK mice showed reduced tumor dissemination. In imatinib treated *CD4*-NPM-ALK-*CD4*$^{\Delta\Delta JUN}$ tumor cell dissemination to other organs was completely blocked. We assumed that changes in tumor vasculature could be involved. Immunohistochemical analysis for the stromal factors CD31, alpha-smooth muscle actin, collagen IV, vimentin and S100A/B revealed that expression of these factors was reduced in *CD4*-NPM-ALK-*CD4*$^{\Delta\Delta JUN}$ and imatinib treated mice compared to untreated NPM-ALK mice. Therefore we suppose that blockage of PDGFRB by imatinib affects both, cancer cells and the tumor stroma. The tumor stroma contributes to tumor growth and dissemination and consists of different factors such as microvessels, inflammatory cells, ECM, CAFs (also referred as myofibroblasts) and smooth muscle cells.[75,151] PDGFRB is known to be partly involved in the regulation of myofibroblasts, which are known to be prominent modifiers of tumor progression.[152] In contrast to normal fibroblasts, CAFs can promote tumor growth and can modulate the tumorigenic properties of neoplastic cells.[153] The blockage of PDGFRB by imatinib was shown to severely reduce expression of alpha-SMA, a marker for myofibroblasts, indicating that the tumor stroma was not as reactive as in untreated mice.

As shown by vimentin and S100A/B staining, there were significantly more stromal fibroblasts in untreated *CD4*-NPM-ALK lymphomas compared to imatinib treated lymphomas. Stromal fibroblasts have important roles in regulating the ECM and produce paracrine factors contributing to cell proliferation, survival and death. Staining for Collagen IV, which is one of the most abundant proteins in the extracellular matrix, revealed that its expression is significantly reduced in imatinib treated *CD4*-NPM-ALK lymphoma samples. Concordant with our data, studies have demonstrated that paracrine activation of PDGF receptors on fibroblasts contribute to tumor stroma recruitment.[101]

Treatment with imatinib also reduced microvessel density (as shown by CD31 staining) in NPM-ALK tumors. Inhibition of PDGFR signaling is supposed to destabilize the tumor vasculature by decreasing pericyte abundance and attachment to endothelial cells.[154,155]

In summary we could show that blockage of PDGFRB, whether indirect or directly, also affects the tumor stroma. We suppose that both, malignant cells and tumor stroma contribute to tumor progression.

The reason for reduced tumor cell dissemination in imatinib treated *CD4*-NPM-ALK and in *CD4*-NPM-ALK-*CD4*$^{\Delta\Delta JUN}$ mice might be the destabilization of the tumor vasculature. The additional effect of imatinib on the tumor stroma could be the reason for the complete blockage of tumor cell dissemination in treated CD4-NPM-ALK-*CD4*$^{\Delta\Delta JUN}$ mice.

Studies provide evidence, that metastatic, invasive T-cell lymphoma cell lines perform active shape changes in contrast to non-malignant cell lines. [109] They extend pseudopodia, which are a prerequisite for the infiltration of cells into tissues.[109] The correlation between malignant behavior of cancer cells and cell motility parameters, led us to the question, whether they are differentially expressed in *CD4*-NPM-ALK-*CD4*$^{\Delta\Delta JUN}$ lymphomas and imatinib treated *CD4*-NPM-ALK lymphomas compared to untreated *CD4*-NPM-ALK lymphomas.

Our data indicate that there are no statistically significant differences between the expression of pERK, ERK, Paxillin, ROCK-1, ARP2/3, pMLC2, MLC2, pMYPT1, MYPT1 and pAkt in imatinib treated and untreated *CD4*-NPM-ALK lymphomas.

CD4-NPM-ALK-*CD4*$^{\Delta\Delta JUN}$ lymphomas showed a significantly increased expression of phosphorylated ERK1/2, although expression of ERK1/2 was reduced. The ERK pathway is activated by growth factors and is often deregulated in cancer. There is evidence that the pathway promotes cell proliferation, cell survival and metastasis. Studies reveal that p-ERK1/2 overexpression is correlated with decreased survival and poor prognosis in many cancer types. [156-158], but it also appears to have favorable effects on patient survival in cancers like adenocarcinoma of the endometrium.[159] We suppose that the high activation of ERK1/2 might be due to the disruption of a negative feedback loop in *CD4*-NPM-ALK-*CD4*$^{\Delta\Delta JUN}$ lymphomas. Recent evidence suggests the existence of a cross-talk between the JNK pathway and the ERK pathway. [160] Sustained activation of the JNK-JUN pathway resulted in attenuation of the mitogen-activated ERK pathway.[160]

Furthermore we found, that expression of ARP2/3 was significantly reduced in *CD4*-NPM-ALK-*CD4*$^{\Delta\Delta JUN}$ lymphomas and slightly reduced in imatinib treated *CD4*-NPM-ALK lymphomas compared to untreated *CD4*-NPM-ALK lymphomas. The ARP2/3 complex is a central player in regulation actin polymerization, which is a prerequisite for cellular movement. A study revealed that metastatic, invasive variants of lymphoma cell lines protrude and retract pseudopodia in contrast to noninvasive cell lines. It was shown that a high level of actin polymerization correlates with infiltration of the cells into tissues.[109] Recent evidence suggests that ERK plays a role in the activation of ARP2/3 by phosphorylating components of the WAVE2 Regulatory Complex (WRC). WRC activation leads to Arp2/3 binding and generation of the actin meshwork, providing the pushing force for protrusion initiation. [161]

The reduced expression of ARP2/3 in *CD4*-NPM-ALK-*CD4*$^{\Delta\Delta JUN}$ lymphomas is consistent with the fact that these lymphomas show reduced tumor cell dissemination into other organs.

Furthermore we found that the expression of ROCK1 and Paxillin was reduced in *CD4*-NPM-ALK-*CD4*$^{\Delta\Delta JUN}$ lymphomas, whereas their expression was elevated in treated lymphomas compared to untreated samples. ROCK1 contributes to cell motility in many ways, for example by phosphorylating MLC2.[118] Paxillin is a regulator of the Rho family of small GTPases, which play important roles in cell contractility, cell polarization and the formation of filopodia.[113] Paxillin was shown to be activated by various kinases including JNK [114] and ERK1/2.[162]

The expression of MLC2 appears to be contradictory, since it is increased in *CD4*-NPM-ALK-*CD4*$^{\Delta\Delta JUN}$ lymphomas. MLC2 is activated by ROCK [118] and plays a role in the disassembly of cell-matrix adhesions at the rear of migrating cells. [121]

Furthermore our data indicate that Akt activation is increased in *CD4*-NPM-ALK-*CD4*$^{\Delta\Delta JUN}$ lymphomas and treated lymphomas compared to *CD4*-NPM-ALK lymphomas. Akt has been shown to be required for chemotaxis in mammalian leukocytes. [163] Clinical studies revealed that increased Akt expression in tumors of cancer patients correlates with more invasive and metastatic diseases. However, recent studies demonstrated an anti-migratory and anti-invasive role for Akt in human breast cancer cell lines[164] and in a transgenic mammary mouse model.[165]

Akt regulates actin organization and cell motility via various substrates. Girdin, an actin binding protein, was found to be phosphorylated by Akt. Phosphorylated Girdin accumulates at the leading edge of migrating cells, where it plays a role in the formation of lamellipodia.[124] Another potential target of Akt proteins in cell migration, glycogen synthase kinase-3 (GSK-3), is inhibited by Akt phosphorylation.[166] It was shown that downregulation of GSK-3 or h-prune, a GSK-3 interacting protein, effectively inhibited cell motility by suppressing the activation of the focal adhesion kinase (FAK) and Rac, as well as the disassembly of Paxillin.[167]

MYPT1 is a myosin light chain binding subunit (MBS) that controls dephosphorylation of MLC2.[123] Phosphorylation of MYPT1 on Threonine 696 inhibits phosphatase activity. [168] Kinases that have been reported to phosphorylate MYPT1 include ROCK1 and ROCK2.[168] In relation to MYPT1 expression, we found that levels of pMYPT1 were reduced in *CD4*-NPM-ALK-*CD4*$^{\Delta\Delta JUN}$ samples indicating that it is more activated in these lymphomas. Reduced levels of pMYPT1 may result in lower levels of pMLC2, since MYPT1 controls dephosphorylation of pMLC2. However, we found that pMLC2 levels were elevated in *CD4*-NPM-ALK-*CD4*$^{\Delta\Delta JUN}$ lymphomas.

Since phosphorylation of MLC2 plays an important role in the actomyosin contractility [121], we would have expected reduced levels of pMLC2 in *CD4*-NPM-ALK-*CD4*$^{\Delta\Delta JUN}$ lymphomas.

However, due to the limited sample size and tumor heterogeneity, the standard variations were relatively high and therefore the results were of only limited informative value. More tumor samples will have to be analyzed in the future to get.

In conclusion we could show that the tyrosine kinase inhibitor imatinib has a growth inhibitory effect on mouse ALK$^+$ ALCL cell lines *in vitro* as well as on engrafted murine ALK$^+$ ALCL tumors in SCID mice. In the transgenic *CD4*-NPM-ALK mouse model we could demonstrate that the blockage of PDGFRB by imatinib not only affects the lymphoma cells, but also the tumor stroma. We propose that impairment of PDGFRB signaling followed by destabilization of the tumor stroma in *CD4*-NPM-ALK-*CD4*$^{\Delta\Delta JUN}$ lymphomas as well as in imatinib treated *CD4*-NPM-ALK lymphomas might play an essential role in the reduced tumor cell dissemination observed.

7 References

1. Delsol, G. [The 2008 WHO lymphoma classification]. *Ann Pathol* 28 Spec No 1, S20-24, (2008)

2. Kuppers, R., Schwering, I., Brauninger, A., Rajewsky, K. & Hansmann, M. L. Biology of Hodgkin's lymphoma. *Ann Oncol* 13 Suppl 1, 11-18, (2002)

3. Shankland, K. R., Armitage, J. O. & Hancock, B. W. Non-Hodgkin lymphoma. *Lancet*, (2012)

4. Evans, L. S. & Hancock, B. W. Non-Hodgkin lymphoma. *Lancet* 362, 139-146, (2003)

5. Vega, F. & Medeiros, L. J. Chromosomal translocations involved in non-Hodgkin lymphomas. *Arch Pathol Lab Med* 127, 1148-1160, (2003)

6. Neri, A., Barriga, F., Knowles, D. M., Magrath, I. T. & Dalla-Favera, R. Different regions of the immunoglobulin heavy-chain locus are involved in chromosomal translocations in distinct pathogenetic forms of Burkitt lymphoma. *Proc Natl Acad Sci U S A* 85, 2748-2752, (1988)

7. Papadopoulos, P., Ridge, S. A., Boucher, C. A., Stocking, C. & Wiedemann, L. M. The novel activation of ABL by fusion to an ets-related gene, TEL. *Cancer Res* 55, 34-38, (1995)

8. Kurzrock, R., Shtalrid, M., Talpaz, M., Kloetzer, W. S. & Gutterman, J. U. Expression of c-abl in Philadelphia-positive acute myelogenous leukemia. *Blood* 70, 1584-1588, (1987)

9. Kurzrock, R. *et al.* A novel c-abl protein product in Philadelphia-positive acute lymphoblastic leukaemia. *Nature* 325, 631-635, (1987)

10. Lamant, L., Dastugue, N., Pulford, K., Delsol, G. & Mariame, B. A new fusion gene TPM3-ALK in anaplastic large cell lymphoma created by a (1;2)(q25;p23) translocation. *Blood* 93, 3088-3095, (1999)

11. Hernandez, L. *et al.* TRK-fused gene (TFG) is a new partner of ALK in anaplastic large cell lymphoma producing two structurally different TFG-ALK translocations. *Blood* 94, 3265-3268, (1999)

12. Lamant, L. *et al.* High incidence of the t(2;5)(p23;q35) translocation in anaplastic large cell lymphoma and its lack of detection in Hodgkin's disease. Comparison of cytogenetic analysis, reverse transcriptase-polymerase chain reaction, and P-80 immunostaining. *Blood* 87, 284-291, (1996)

13. Stein, H. *et al.* The expression of the Hodgkin's disease associated antigen Ki-1 in reactive and neoplastic lymphoid tissue: evidence that Reed-Sternberg cells and histiocytic malignancies are derived from activated lymphoid cells. *Blood* 66, 848-858, (1985)

14. O'Connor, N. T. *et al.* Genotypic analysis of large cell lymphomas which express the Ki-1 antigen. *Histopathology* 11, 733-740, (1987)

15. Chott, A. *et al.* Ki-1-positive large cell lymphoma. A clinicopathologic study of 41 cases. *Am J Surg Pathol* 14, 439-448, (1990)

16. Savage, K. J. *et al.* ALK- anaplastic large-cell lymphoma is clinically and immunophenotypically different from both ALK+ ALCL and peripheral T-cell lymphoma, not otherwise specified: report from the International Peripheral T-Cell Lymphoma Project. *Blood* 111, 5496-5504, (2008)

17. Benharroch, D. *et al.* ALK-positive lymphoma: a single disease with a broad spectrum of morphology. *Blood* 91, 2076-2084, (1998)

18. Morris, S. W. *et al.* Fusion of a kinase gene, ALK, to a nucleolar protein gene, NPM, in non-Hodgkin's lymphoma. *Science* 263, 1281-1284, (1994)

19. Chiarle, R., Voena, C., Ambrogio, C., Piva, R. & Inghirami, G. The anaplastic lymphoma kinase in the pathogenesis of cancer. *Nat Rev Cancer* 8, 11-23, (2008)

20. Gandhi, L. & Janne, P. A. Crizotinib for ALK-rearranged non-small cell lung cancer: a new targeted therapy for a new target. *Clin Cancer Res* 18, 3737-3742, (2012)

21. Galkin, A. V. *et al.* Identification of NVP-TAE684, a potent, selective, and efficacious inhibitor of NPM-ALK. *Proc Natl Acad Sci U S A* 104, 270-275, (2007)

22. Laimer, D. *et al.* PDGFR blockade is a rational and effective therapy for NPM-ALK-driven lymphomas. *Nat Med*, (2012)

23. Tian, M., Chang, T., Merkel, K. D. & Babbitt, W. R. Reconfiguration of spectral absorption features using a frequency-chirped laser pulse. *Appl Opt* 50, 6548-6554, (2011)

24. Kuefer, M. U. *et al.* Retrovirus-mediated gene transfer of NPM-ALK causes lymphoid malignancy in mice. *Blood* 90, 2901-2910, (1997)

25. Morris, S. W. *et al.* ALK, the chromosome 2 gene locus altered by the t(2;5) in non-Hodgkin's lymphoma, encodes a novel neural receptor tyrosine kinase that is highly related to leukocyte tyrosine kinase (LTK). *Oncogene* 14, 2175-2188, (1997)

26. Iwahara, T. *et al.* Molecular characterization of ALK, a receptor tyrosine kinase expressed specifically in the nervous system. *Oncogene* 14, 439-449, (1997)

27. Borer, R. A., Lehner, C. F., Eppenberger, H. M. & Nigg, E. A. Major nucleolar proteins shuttle between nucleus and cytoplasm. *Cell* 56, 379-390, (1989)

28. Chan, P. K. & Chan, F. Y. Nucleophosmin/B23 (NPM) oligomer is a major and stable entity in HeLa cells. *Biochim Biophys Acta* 1262, 37-42, (1995)

29. Beylot-Barry, M., Groppi, A., Vergier, B., Pulford, K. & Merlio, J. P. Characterization of t(2;5) reciprocal transcripts and genomic breakpoints in CD30+ cutaneous lymphoproliferations. *Blood* 91, 4668-4676, (1998)

30. Bischof, D., Pulford, K., Mason, D. Y. & Morris, S. W. Role of the nucleophosmin (NPM) portion of the non-Hodgkin's lymphoma-associated NPM-anaplastic

lymphoma kinase fusion protein in oncogenesis. *Mol Cell Biol* 17, 2312-2325, (1997)

31. Amin, H. M. & Lai, R. Pathobiology of ALK+ anaplastic large-cell lymphoma. *Blood* 110, 2259-2267, (2007)

32. Crockett, D. K., Lin, Z., Elenitoba-Johnson, K. S. & Lim, M. S. Identification of NPM-ALK interacting proteins by tandem mass spectrometry. *Oncogene* 23, 2617-2629, (2004)

33. Chiarle, R. *et al.* Stat3 is required for ALK-mediated lymphomagenesis and provides a possible therapeutic target. *Nat Med* 11, 623-629, (2005)

34. Bai, R. Y. *et al.* Nucleophosmin-anaplastic lymphoma kinase associated with anaplastic large-cell lymphoma activates the phosphatidylinositol 3-kinase/Akt antiapoptotic signaling pathway. *Blood* 96, 4319-4327, (2000)

35. Slupianek, A. *et al.* Role of phosphatidylinositol 3-kinase-Akt pathway in nucleophosmin/anaplastic lymphoma kinase-mediated lymphomagenesis. *Cancer Res* 61, 2194-2199, (2001)

36. Mathas, S. *et al.* Aberrantly expressed c-Jun and JunB are a hallmark of Hodgkin lymphoma cells, stimulate proliferation and synergize with NF-kappa B. *EMBO J* 21, 4104-4113, (2002)

37. Gu, T. L. *et al.* NPM-ALK fusion kinase of anaplastic large-cell lymphoma regulates survival and proliferative signaling through modulation of FOXO3a. *Blood* 103, 4622-4629, (2004)

38. Singh, R. R. *et al.* Sonic hedgehog signaling pathway is activated in ALK-positive anaplastic large cell lymphoma. *Cancer Res* 69, 2550-2558, (2009)

39. Chiarle, R. *et al.* NPM-ALK transgenic mice spontaneously develop T-cell lymphomas and plasma cell tumors. *Blood* 101, 1919-1927, (2003)

40. Zamo, A. *et al.* Anaplastic lymphoma kinase (ALK) activates Stat3 and protects hematopoietic cells from cell death. *Oncogene* 21, 1038-1047, (2002)

41. Khoury, J. D. *et al.* Differential expression and clinical significance of tyrosine-phosphorylated STAT3 in ALK+ and ALK- anaplastic large cell lymphoma. *Clin Cancer Res* 9, 3692-3699, (2003)

42. Amin, H. M. *et al.* Selective inhibition of STAT3 induces apoptosis and G(1) cell cycle arrest in ALK-positive anaplastic large cell lymphoma. *Oncogene* 23, 5426-5434, (2004)

43. Pulford, K., Morris, S. W. & Turturro, F. Anaplastic lymphoma kinase proteins in growth control and cancer. *J Cell Physiol* 199, 330-358, (2004)

44. Turner, S. D., Tooze, R., Maclennan, K. & Alexander, D. R. Vav-promoter regulated oncogenic fusion protein NPM-ALK in transgenic mice causes B-cell lymphomas with hyperactive Jun kinase. *Oncogene* 22, 7750-7761, (2003)

45. Eferl, R. & Wagner, E. F. AP-1: a double-edged sword in tumorigenesis. *Nat Rev Cancer* 3, 859-868, (2003)

46. Watanabe, M. *et al.* JunB induced by constitutive CD30-extracellular signal-regulated kinase 1/2 mitogen-activated protein kinase signaling activates the CD30 promoter in anaplastic large cell lymphoma and reed-sternberg cells of Hodgkin lymphoma. *Cancer Res* 65, 7628-7634, (2005)

47. Bai, R. Y., Dieter, P., Peschel, C., Morris, S. W. & Duyster, J. Nucleophosmin-anaplastic lymphoma kinase of large-cell anaplastic lymphoma is a constitutively active tyrosine kinase that utilizes phospholipase C-gamma to mediate its mitogenicity. *Mol Cell Biol* 18, 6951-6961, (1998)

48. Shaulian, E. & Karin, M. AP-1 as a regulator of cell life and death. *Nat Cell Biol* 4, E131-136, (2002)

49. Shaulian, E. AP-1--The Jun proteins: Oncogenes or tumor suppressors in disguise? *Cell Signal* 22, 894-899, (2010)

50. Karin, M., Liu, Z. & Zandi, E. AP-1 function and regulation. *Curr Opin Cell Biol* 9, 240-246, (1997)

51. Leppa, S. & Bohmann, D. Diverse functions of JNK signaling and c-Jun in stress response and apoptosis. *Oncogene* 18, 6158-6162, (1999)

52. Shaulian, E. & Karin, M. AP-1 in cell proliferation and survival. *Oncogene* 20, 2390-2400, (2001)

53. Wisdom, R. AP-1: one switch for many signals. *Exp Cell Res* 253, 180-185, (1999)

54. Rassidakis, G. Z. *et al.* JunB expression is a common feature of CD30+ lymphomas and lymphomatoid papulosis. *Mod Pathol* 18, 1365-1370, (2005)

55. Staber, P. B. *et al.* The oncoprotein NPM-ALK of anaplastic large-cell lymphoma induces JUNB transcription via ERK1/2 and JunB translation via mTOR signaling. *Blood* 110, 3374-3383, (2007)

56. Drakos, E. *et al.* c-Jun expression and activation are restricted to CD30+ lymphoproliferative disorders. *Am J Surg Pathol* 31, 447-453, (2007)

57. Leventaki, V. *et al.* NPM-ALK oncogenic kinase promotes cell-cycle progression through activation of JNK/cJun signaling in anaplastic large-cell lymphoma. *Blood* 110, 1621-1630, (2007)

58. Lamb, R. F. *et al.* AP-1-mediated invasion requires increased expression of the hyaluronan receptor CD44. *Mol Cell Biol* 17, 963-976, (1997)

59. Toft, D. J., Rosenberg, S. B., Bergers, G., Volpert, O. & Linzer, D. I. Reactivation of proliferin gene expression is associated with increased angiogenesis in a cell culture model of fibrosarcoma tumor progression. *Proc Natl Acad Sci U S A* 98, 13055-13059, (2001)

60. Heldin, C. H. & Westermark, B. Mechanism of action and in vivo role of platelet-derived growth factor. *Physiol Rev* 79, 1283-1316, (1999)

61. Andrae, J., Gallini, R. & Betsholtz, C. Role of platelet-derived growth factors in physiology and medicine. *Genes Dev* 22, 1276-1312, (2008)

62. Williams, L. T. Signal transduction by the platelet-derived growth factor receptor. *Science* 243, 1564-1570, (1989)

63. Claesson-Welsh, L. Signal transduction by the PDGF receptors. *Prog Growth Factor Res* 5, 37-54, (1994)

64. Hu, Q., Klippel, A., Muslin, A. J., Fantl, W. J. & Williams, L. T. Ras-dependent induction of cellular responses by constitutively active phosphatidylinositol-3 kinase. *Science* 268, 100-102, (1995)

65. Seger, R. & Krebs, E. G. The MAPK signaling cascade. *FASEB J* 9, 726-735, (1995)

66. Kundra, V. *et al.* Regulation of chemotaxis by the platelet-derived growth factor receptor-beta. *Nature* 367, 474-476, (1994)

67. Soriano, P. Abnormal kidney development and hematological disorders in PDGF beta-receptor mutant mice. *Genes Dev* 8, 1888-1896, (1994)

68. Soriano, P. The PDGF alpha receptor is required for neural crest cell development and for normal patterning of the somites. *Development* 124, 2691-2700, (1997)

69. Kenner, L. *et al.* Mice lacking JunB are osteopenic due to cell-autonomous osteoblast and osteoclast defects. *J Cell Biol* 164, 613-623, (2004)

70. Behrens, A. *et al.* Impaired postnatal hepatocyte proliferation and liver regeneration in mice lacking c-jun in the liver. *EMBO J* 21, 1782-1790, (2002)

71. Wolfer, A. *et al.* Inactivation of Notch 1 in immature thymocytes does not perturb CD4 or CD8T cell development. *Nat Immunol* 2, 235-241, (2001)

72. Dvorak, H. F., Nagy, J. A. & Dvorak, A. M. Structure of solid tumors and their vasculature: implications for therapy with monoclonal antibodies. *Cancer Cells* 3, 77-85, (1991)

73. Folkman, J. Tumor angiogenesis: therapeutic implications. *N Engl J Med* 285, 1182-1186, (1971)

74. Anton, K. & Glod, J. Targeting the tumor stroma in cancer therapy. *Curr Pharm Biotechnol* 10, 185-191, (2009)

75. Kufe DW, P. R., Weichselbaum RR, et al., editors. *Holland-Frei Cancer Medicine*. 6th edition edn, (BC Decker, 2003).

76. Rapin, V. *et al.* Medullary breast carcinoma. A reevaluation of 95 cases of breast cancer with inflammatory stroma. *Cancer* 61, 2503-2510, (1988)

77. Mueller, M. M. & Fusenig, N. E. Friends or foes - bipolar effects of the tumour stroma in cancer. *Nat Rev Cancer* 4, 839-849, (2004)

78. Carmeliet, P. & Jain, R. K. Angiogenesis in cancer and other diseases. *Nature* 407, 249-257, (2000)

79. Lindahl, P., Johansson, B. R., Leveen, P. & Betsholtz, C. Pericyte loss and microaneurysm formation in PDGF-B-deficient mice. *Science* 277, 242-245, (1997)

80. Apte, S. M., Fan, D., Killion, J. J. & Fidler, I. J. Targeting the platelet-derived growth factor receptor in antivascular therapy for human ovarian carcinoma. *Clin Cancer Res* 10, 897-908, (2004)

81. Sundberg, C., Ljungstrom, M., Lindmark, G., Gerdin, B. & Rubin, K. Microvascular pericytes express platelet-derived growth factor-beta receptors in human healing wounds and colorectal adenocarcinoma. *Am J Pathol* 143, 1377-1388, (1993)

82. Abramsson, A. *et al.* Analysis of mural cell recruitment to tumor vessels. *Circulation* 105, 112-117, (2002)

83. Morikawa, S. *et al.* Abnormalities in pericytes on blood vessels and endothelial sprouts in tumors. *Am J Pathol* 160, 985-1000, (2002)

84. Guo, P. *et al.* Platelet-derived growth factor-B enhances glioma angiogenesis by stimulating vascular endothelial growth factor expression in tumor endothelia and by promoting pericyte recruitment. *Am J Pathol* 162, 1083-1093, (2003)

85. Abramsson, A., Lindblom, P. & Betsholtz, C. Endothelial and nonendothelial sources of PDGF-B regulate pericyte recruitment and influence vascular pattern formation in tumors. *J Clin Invest* 112, 1142-1151, (2003)

86. Furuhashi, M. *et al.* Platelet-derived growth factor production by B16 melanoma cells leads to increased pericyte abundance in tumors and an associated increase in tumor growth rate. *Cancer Res* 64, 2725-2733, (2004)

87. Tlsty, T. D. Stromal cells can contribute oncogenic signals. *Semin Cancer Biol* 11, 97-104, (2001)

88. Allinen, M. *et al.* Molecular characterization of the tumor microenvironment in breast cancer. *Cancer Cell* 6, 17-32, (2004)

89. Park, J. E. *et al.* Fibroblast activation protein, a dual specificity serine protease expressed in reactive human tumor stromal fibroblasts. *J Biol Chem* 274, 36505-36512, (1999)

90. Tlsty, T. D. & Coussens, L. M. Tumor stroma and regulation of cancer development. *Annu Rev Pathol* 1, 119-150, (2006)

91. Chauhan, H. *et al.* There is more than one kind of myofibroblast: analysis of CD34 expression in benign, in situ, and invasive breast lesions. *J Clin Pathol* 56, 271-276, (2003)

92. Olumi, A. F. *et al.* Carcinoma-associated fibroblasts direct tumor progression of initiated human prostatic epithelium. *Cancer Res* 59, 5002-5011, (1999)

93. Lohr, M. *et al.* Transforming growth factor-beta1 induces desmoplasia in an experimental model of human pancreatic carcinoma. *Cancer Res* 61, 550-555, (2001)

94. De Wever, O. & Mareel, M. Role of tissue stroma in cancer cell invasion. *J Pathol* 200, 429-447, (2003)

95. Shao, Z. M., Nguyen, M. & Barsky, S. H. Human breast carcinoma desmoplasia is PDGF initiated. *Oncogene* 19, 4337-4345, (2000)

96. Bhardwaj, B. *et al.* Localization of platelet-derived growth factor beta receptor expression in the periepithelial stroma of human breast carcinoma. *Clin Cancer Res* 2, 773-782, (1996)

97. Kawai, T., Hiroi, S. & Torikata, C. Expression in lung carcinomas of platelet-derived growth factor and its receptors. *Lab Invest* 77, 431-436, (1997)

98. Ebert, M. *et al.* Induction of platelet-derived growth factor A and B chains and over-expression of their receptors in human pancreatic cancer. *Int J Cancer* 62, 529-535, (1995)

99. Funa, K. *et al.* Expression of platelet-derived growth factor beta-receptors on stromal tissue cells in human carcinoid tumors. *Cancer Res* 50, 748-753, (1990)

100. Skobe, M. & Fusenig, N. E. Tumorigenic conversion of immortal human keratinocytes through stromal cell activation. *Proc Natl Acad Sci U S A* 95, 1050-1055, (1998)

101. Forsberg, K., Valyi-Nagy, I., Heldin, C. H., Herlyn, M. & Westermark, B. Platelet-derived growth factor (PDGF) in oncogenesis: development of a vascular connective tissue stroma in xenotransplanted human melanoma producing PDGF-BB. *Proc Natl Acad Sci U S A* 90, 393-397, (1993)

102. Jechlinger, M. *et al.* Autocrine PDGFR signaling promotes mammary cancer metastasis. *J Clin Invest* 116, 1561-1570, (2006)

103. Seymour, L., Dajee, D. & Bezwoda, W. R. Tissue platelet derived-growth factor (PDGF) predicts for shortened survival and treatment failure in advanced breast cancer. *Breast Cancer Res Treat* 26, 247-252, (1993)

104. Cao, R. *et al.* PDGF-BB induces intratumoral lymphangiogenesis and promotes lymphatic metastasis. *Cancer Cell* 6, 333-345, (2004)

105. Gabarre, J., Bikandou, B. & Binet, J. L. [Sites of lymphomas]. *Rev Prat* 43, 1633-1639, (1993)

106. Scheimberg, I. B. *et al.* Pathology of the liver in leukaemia and lymphoma. A study of 110 autopsies. *Histopathology* 26, 311-321, (1995)

107. Ananthakrishnan, R. & Ehrlicher, A. The forces behind cell movement. *Int J Biol Sci* 3, 303-317, (2007)

108. Doyle, G. M., Sharief, Y. & Mohler, J. L. Prediction of metastatic potential by cancer cell motility in the Dunning R-3327 prostatic adenocarcinoma in vivo model. *J Urol* 147, 514-518, (1992)

109. Verschueren, H., Van der Taelen, I., Dewit, J., De Braekeleer, J. & De Baetselier, P. Metastatic competence of BW5147 T-lymphoma cell lines is correlated with in vitro invasiveness, motility and F-actin content. *J Leukoc Biol* 55, 552-556, (1994)

110. Ridley, A. J. Rho GTPases and cell migration. *J Cell Sci* 114, 2713-2722, (2001)

111. Viala, E. & Pouyssegur, J. Regulation of tumor cell motility by ERK mitogen-activated protein kinases. *Ann N Y Acad Sci* 1030, 208-218, (2004)

112. Deakin, N. O. & Turner, C. E. Paxillin comes of age. *J Cell Sci* 121, 2435-2444, (2008)

113. Raftopoulou, M. & Hall, A. Cell migration: Rho GTPases lead the way. *Dev Biol* 265, 23-32, (2004)

114. Huang, C., Rajfur, Z., Borchers, C., Schaller, M. D. & Jacobson, K. JNK phosphorylates paxillin and regulates cell migration. *Nature* 424, 219-223, (2003)

115. Ishibe, S., Joly, D., Zhu, X. & Cantley, L. G. Phosphorylation-dependent paxillin-ERK association mediates hepatocyte growth factor-stimulated epithelial morphogenesis. *Mol Cell* 12, 1275-1285, (2003)

116. Riento, K. & Ridley, A. J. Rocks: multifunctional kinases in cell behaviour. *Nat Rev Mol Cell Biol* 4, 446-456, (2003)

117. Nakagawa, O. *et al.* ROCK-I and ROCK-II, two isoforms of Rho-associated coiled-coil forming protein serine/threonine kinase in mice. *FEBS Lett* 392, 189-193, (1996)

118. Amano, M. *et al.* Phosphorylation and activation of myosin by Rho-associated kinase (Rho-kinase). *J Biol Chem* 271, 20246-20249, (1996)

119. Kawano, Y. *et al.* Phosphorylation of myosin-binding subunit (MBS) of myosin phosphatase by Rho-kinase in vivo. *J Cell Biol* 147, 1023-1038, (1999)

120. Olson, M. F. & Sahai, E. The actin cytoskeleton in cancer cell motility. *Clin Exp Metastasis* 26, 273-287, (2009)

121. Somlyo, A. P. & Somlyo, A. V. Signal transduction by G-proteins, rho-kinase and protein phosphatase to smooth muscle and non-muscle myosin II. *J Physiol* 522 Pt 2, 177-185, (2000)

122. Zeng, Q. *et al.* Endothelial cell retraction is induced by PAK2 monophosphorylation of myosin II. *J Cell Sci* 113 (Pt 3), 471-482, (2000)

123. Ito, M., Nakano, T., Erdodi, F. & Hartshorne, D. J. Myosin phosphatase: structure, regulation and function. *Mol Cell Biochem* 259, 197-209, (2004)

124. Enomoto, A. *et al.* Akt/PKB regulates actin organization and cell motility via Girdin/APE. *Dev Cell* 9, 389-402, (2005)

125. Chin, Y. R. & Toker, A. Function of Akt/PKB signaling to cell motility, invasion and the tumor stroma in cancer. *Cell Signal* 21, 470-476, (2009)

126. Druker, B. J. & Lydon, N. B. Lessons learned from the development of an abl tyrosine kinase inhibitor for chronic myelogenous leukemia. *J Clin Invest* 105, 3-7, (2000)

127. Buchdunger, E., Matter, A. & Druker, B. J. Bcr-Abl inhibition as a modality of CML therapeutics. *Biochim Biophys Acta* 1551, M11-18, (2001)

128. Savage, D. G. & Antman, K. H. Imatinib mesylate--a new oral targeted therapy. *N Engl J Med* 346, 683-693, (2002)

129. Rubin, B. P. *et al.* Molecular targeting of platelet-derived growth factor B by imatinib mesylate in a patient with metastatic dermatofibrosarcoma protuberans. *J Clin Oncol* 20, 3586-3591, (2002)

130. Wang, H. *et al.* Imatinib mesylate (STI-571) enhances antigen-presenting cell function and overcomes tumor-induced CD4+ T-cell tolerance. *Blood* 105, 1135-1143, (2005)

131. Seggewiss, R. *et al.* Imatinib inhibits T-cell receptor-mediated T-cell proliferation and activation in a dose-dependent manner. *Blood* 105, 2473-2479, (2005)

132. Dietz, A. B. *et al.* Imatinib mesylate inhibits T-cell proliferation in vitro and delayed-type hypersensitivity in vivo. *Blood* 104, 1094-1099, (2004)

133. Weisberg, E. *et al.* Characterization of AMN107, a selective inhibitor of native and mutant Bcr-Abl. *Cancer Cell* 7, 129-141, (2005)

134. Laimer, D. *et al.* PDGFR blockade is a rational and effective therapy for NPM-ALK-driven lymphomas. *Nat Med* 18, 1699-1704, (2012)

135. Fox, S. B. & Harris, A. L. Markers of tumor angiogenesis: clinical applications in prognosis and anti-angiogenic therapy. *Invest New Drugs* 15, 15-28, (1997)

136. Nagamoto, T., Eguchi, G. & Beebe, D. C. Alpha-smooth muscle actin expression in cultured lens epithelial cells. *Invest Ophthalmol Vis Sci* 41, 1122-1129, (2000)

137. Thomas, K. & Mayston, V. Vimentin as a tumour marker. *Histopathology* 11, 991, (1987)

138. Mandal, M. *et al.* Epithelial to mesenchymal transition in head and neck squamous carcinoma: association of Src activation with E-cadherin down-regulation, vimentin expression, and aggressive tumor features. *Cancer* 112, 2088-2100, (2008)

139. Donato, R. S100: a multigenic family of calcium-modulated proteins of the EF-hand type with intracellular and extracellular functional roles. *Int J Biochem Cell Biol* 33, 637-668, (2001)

140. Heizmann, C. W., Fritz, G. & Schafer, B. W. S100 proteins: structure, functions and pathology. *Front Biosci* 7, d1356-1368, (2002)

141. Salama, I., Malone, P. S., Mihaimeed, F. & Jones, J. L. A review of the S100 proteins in cancer. *Eur J Surg Oncol* 34, 357-364, (2008)

142. Bartling, B. *et al.* S100A2-S100P expression profile and diagnosis of non-small cell lung carcinoma: impairment by advanced tumour stages and neoadjuvant chemotherapy. *Eur J Cancer* 43, 1935-1943, (2007)

143. Boye, K. & Maelandsmo, G. M. S100A4 and metastasis: a small actor playing many roles. *Am J Pathol* 176, 528-535, (2010)

144. Ryan, D. G. *et al.* Involvement of S100A4 in stromal fibroblasts of the regenerating cornea. *Invest Ophthalmol Vis Sci* 44, 4255-4262, (2003)

145. Rehman, I. *et al.* Dysregulated expression of S100A11 (calgizzarin) in prostate cancer and precursor lesions. *Hum Pathol* 35, 1385-1391, (2004)

146. Rust, R. *et al.* High expression of calcium-binding proteins, S100A10, S100A11 and CALM2 in anaplastic large cell lymphoma. *Br J Haematol* 131, 596-608, (2005)

147. Rowley, J. D. Letter: A new consistent chromosomal abnormality in chronic myelogenous leukaemia identified by quinacrine fluorescence and Giemsa staining. *Nature* 243, 290-293, (1973)

148. Druker, B. J. Inhibition of the Bcr-Abl tyrosine kinase as a therapeutic strategy for CML. *Oncogene* 21, 8541-8546, (2002)

149. Dan, S., Naito, M. & Tsuruo, T. Selective induction of apoptosis in Philadelphia chromosome-positive chronic myelogenous leukemia cells by an inhibitor of BCR - ABL tyrosine kinase, CGP 57148. *Cell Death Differ* 5, 710-715, (1998)

150. Rix, U. *et al.* Chemical proteomic profiles of the BCR-ABL inhibitors imatinib, nilotinib, and dasatinib reveal novel kinase and nonkinase targets. *Blood* 110, 4055-4063, (2007)

151. Hanahan, D. & Coussens, L. M. Accessories to the crime: functions of cells recruited to the tumor microenvironment. *Cancer Cell* 21, 309-322, (2012)

152. Kitadai, Y. Angiogenesis and lymphangiogenesis of gastric cancer. *J Oncol* 2010, 468725, (2010)

153. Micke, P. & Ostman, A. Exploring the tumour environment: cancer-associated fibroblasts as targets in cancer therapy. *Expert Opin Ther Targets* 9, 1217-1233, (2005)

154. Bergers, G., Song, S., Meyer-Morse, N., Bergsland, E. & Hanahan, D. Benefits of targeting both pericytes and endothelial cells in the tumor vasculature with kinase inhibitors. *J Clin Invest* 111, 1287-1295, (2003)

155. Ribatti, D., Nico, B., Crivellato, E., Roccaro, A. M. & Vacca, A. The history of the angiogenic switch concept. *Leukemia* 21, 44-52, (2007)

156. Li, Q. & Yang, Z. Expression of phospho-ERK1/2 and PI3-K in benign and malignant gallbladder lesions and its clinical and pathological correlations. *J Exp Clin Cancer Res* 28, 65, (2009)

157. Gregorj, C. *et al.* ERK1/2 phosphorylation is an independent predictor of complete remission in newly diagnosed adult acute lymphoblastic leukemia. *Blood* 109, 5473-5476, (2007)

158. Vicent, S. *et al.* ERK1/2 is activated in non-small-cell lung cancer and associated with advanced tumours. *Br J Cancer* 90, 1047-1052, (2004)

159. Mizumoto, Y. *et al.* Activation of ERK1/2 occurs independently of KRAS or BRAF status in endometrial cancer and is associated with favorable prognosis. *Cancer Sci* 98, 652-658, (2007)

160. Shen, Y. H. *et al.* Cross-talk between JNK/SAPK and ERK/MAPK pathways: sustained activation of JNK blocks ERK activation by mitogenic factors. *J Biol Chem* 278, 26715-26721, (2003)

161. Mendoza, M. C. *et al.* ERK-MAPK drives lamellipodia protrusion by activating the WAVE2 regulatory complex. *Mol Cell* 41, 661-671, (2011)

162. Cai, X., Li, M., Vrana, J. & Schaller, M. D. Glycogen synthase kinase 3- and extracellular signal-regulated kinase-dependent phosphorylation of paxillin regulates cytoskeletal rearrangement. *Mol Cell Biol* 26, 2857-2868, (2006)

163. Merlot, S. & Firtel, R. A. Leading the way: Directional sensing through phosphatidylinositol 3-kinase and other signaling pathways. *J Cell Sci* 116, 3471-3478, (2003)

164. Yoeli-Lerner, M. *et al.* Akt blocks breast cancer cell motility and invasion through the transcription factor NFAT. *Mol Cell* 20, 539-550, (2005)

165. Hutchinson, J. N., Jin, J., Cardiff, R. D., Woodgett, J. R. & Muller, W. J. Activation of Akt-1 (PKB-alpha) can accelerate ErbB-2-mediated mammary tumorigenesis but suppresses tumor invasion. *Cancer Res* 64, 3171-3178, (2004)

166. Cross, D. A., Alessi, D. R., Cohen, P., Andjelkovich, M. & Hemmings, B. A. Inhibition of glycogen synthase kinase-3 by insulin mediated by protein kinase B. *Nature* 378, 785-789, (1995)

167. Kobayashi, T. *et al.* Glycogen synthase kinase 3 and h-prune regulate cell migration by modulating focal adhesions. *Mol Cell Biol* 26, 898-911, (2006)

168. Feng, J. *et al.* Inhibitory phosphorylation site for Rho-associated kinase on smooth muscle myosin phosphatase. *J Biol Chem* 274, 37385-37390, (1999)

8 Appendix

8.1 Acknowledgements

During my diploma thesis, I was supported by many people. I am deeply indebted to the following people:

First of all, I want to thank my supervisor at the Medical University of Vienna, **Prof. Dr. Lukas Kenner**, who gave me the opportunity to work on such an exciting and successfully scientific project.

I am very thankful to **Daniela Laimer** for her kindly helpfulness in all situations and interesting discussions.

I also want to thank all my **lab colleagues**, without whom, this experience would have been incomplete.

Special thanks to the **whole team of the Clinical Institute of Pathology** for their helpfulness and the very good working atmosphere.

I want to thank **my parents** for supporting me in realizing my objectives and **my boyfriend Tom** and **my little hero Toni** for their patience, love and support.

Special thanks to **Elfi and Hans**, who care lovingly for Toni and without whom, I would not have found the time to finish my thesis.

8.2 Curriculum vitae

Personal Data

Name	Lena Amenitsch
Address	Austria, [redacted]
E-mail	lena_amenitsch@gmx.at
Birth date	[redacted]
Place of birth	Klagenfurt (Austria)
Nationality	Austria
Family Status	unmarried, 1 son

Education

1996 - 2004	Bundesrealgymnasium Spittal/Drau, Matura 2004
2004 – 2006	Study of Physics and Mathematics, University of Vienna
2006 -	Study of Biology, specialization: Genetics and Microbiology, University of Vienna

Work experience

Jan. 2010 – Feb. 2011	Diploma project at the Medical University of Vienna, Institute of Clinical Pathology, Supervisor: Ao.Univ-Prof.Dr. Lukas Kenner

Publications

Laimer D, Dolznig H, Kollmann K, Vesely P, Schlederer M, Merkel O, Schiefer A, Hassler M, Heider S, **Amenitsch L**, Thallinger C, Staber P, Simonitsch-Klupp I, Artaker M, Lagger S, Turner S, Pileri S, Piccaluga P, Valent P, Messana K, Landra I, Weichhart T, Knapp S, Shehata M, Todaro M, Sexl V, Höfler G, Piva R, Medico E, Ruggeri B, Cheng M, Eferl R, Egger G, Penninger J, Jaeger U, Moriggl R, Inghirami G, Kenner L. *PDGFR blockade is a rational and effective therapy for NPM-ALK-driven lymphomas. Nat Med*, (2012)